

**Feasibility Study for the Preparation of a
Twin-Hole Disposal Configuration
Test at the Mont Terri URL**

MACH-2

Final Report

DBE-TEC
DBE TECHNOLOGY GmbH

**Feasibility Study for the Preparation of a
Twin-Hole Disposal Configuration
Test at the Mont Terri URL**

MACH-2

Final Report

Jobmann, M.; Wolf, J.

DBE TECHNOLOGY GmbH
Eschenstraße 55
D-31224 Peine

August 2009

The research work described in this report was funded by the Federal Ministry of Economics and Technology (BMWi = Bundesministerium für Wirtschaft und Technologie) under contract No. FKZ 02E10508. However, the authors are solely responsible for the contents of this publication.

TABLE OF CONTENTS

Executive Summary	5
1 Introduction and Objectives	6
2 Experimental Setup	8
2.1 Objectives of the TwisT experiment	8
2.2 Location of the TwisT experiment	9
2.3 Conceptual design	10
3 Design Calculations	12
3.1 Continuum Model	12
3.1.1 Geometry	12
3.1.2 Constitutive Models	13
3.1.3 Model Parameters	15
3.1.3.1 Thermal, hydraulic, and mechanical parameters	15
3.1.3.2 Creep model	16
3.1.4 Initial conditions	16
3.1.5 Simulation Workflow	17
3.1.6 Model Layouts	18
3.2 Results	18
3.2.1 Thermal layout	19
3.2.2 Hydro-mechanical layout	24
3.2.2.1 Pore pressure	24
3.2.2.2 States of stress and failure	30
3.2.2.3 Displacements	37
3.2.2.3.1 Displacements in the drift	37
3.2.2.3.2 Displacements in the boreholes	40
3.2.2.4 Pressure	43
4 Measurement Concept and Experiment Schedule	47
4.1 Laboratory investigation of host rock and buffer material	47
4.2 Preparation of the experiment and set-up	48
4.2.1 Drilling of the heater boreholes	48
4.2.2 Geological logging of the heater boreholes	48

4.2.3	Drilling and equipping the monitoring boreholes	48
4.2.4	Fabrication and testing of the heaters	50
4.2.5	Geotechnical measurements in the set-up phase	51
4.2.6	In-situ measurement of the thermal conductivity	51
4.2.7	Installation of heater 1 and of the GB buffer material	52
4.2.8	Microseismic measurements (optional)	52
4.2.9	Installation of heater 2 and of the SB buffer material	53
4.3	Experimentation	53
4.3.1	Heating phase 1	53
4.3.2	Heating phase 2	54
4.3.3	Cooling phase	54
4.3.4	De-installation and follow-up studies	54
5	Modelling Concept for Experiment Analysis	55
5.1	Model design and predictive calculation	55
5.2	Modelling during phase 1 of the experiment	55
5.3	Modelling during phase 2 of the experiment	56
5.4	Modelling during the cooling phase	56
6	Experiment Cost Estimate	57
7	Conclusions of Design Calculations	58
8	References	60

Acknowledgements

We would like to thank Christoph Nussbaum from the Geotechnical Institute in St. Ursanne for his on-site support and for providing all necessary information. Additionally, we thank the Mont Terri Consortium for offering us the opportunity to perform the TwisT experiment at the Mont Terri URL.

Executive Summary

The German Federal Government has announced that research and development activities concerning final repositories for high-level waste are to focus on clay formations as host rock in order to investigate alternatives to salt rock which is favoured in the current reference concept. Within the scope of design calculations for a final repository in clay formations, thermo-hydro-mechanical interaction effects have thus been studied, but only based on numerical calculation. The currently preferred disposal concept is based on the emplacement of heat-generating waste in vertical boreholes with a depth of 50 m maximum. How strongly thermally induced interaction between adjacent emplacement boreholes affects a system of vertical boreholes in claystone has not yet been investigated in-situ. However, these interaction effects need to be considered as in a real repository the emplacement boreholes are drilled successively and, depending on the delivery and necessary cooling-off time of the containers at the interim storage facility, are filled at corresponding intervals.

The main goal of the suggested in-situ experiment is to investigate the THM interaction of two adjacent emplacement boreholes that are filled and heated at different times. The project is to be planned and carried out jointly by DBE TECHNOLOGY GmbH and GRS. The Federal Institute for Geosciences and Natural Resources (BGR) has declared its interest in participating. A location for this experiment has been found at the underground research laboratory in Mont Terri, Switzerland, which is located in an Opalinus-clay formation. The project has been presented to the Mont Terri consortium, and a positive vote to carry out the experiment was obtained. The exact location of the experiment has been set within the so-called "sandy facies" of the rock lab which is similar to the German part of the Opalinus clay.

Since time and costs involved in such a major project cannot be reliably estimated without sufficient information, this feasibility study was carried out to establish a solid basis for the planning and implementation of the project. Detailed design calculation were a major part of this study which allowed the development of a suitable experiment configuration and measurement concept. Based on this information, potential subcontractors that are able and qualified to perform the work were identified, and corresponding quotations necessary for the budget planning were obtained.

As a result, the feasibility of the "Twin hole disposal configuration test" (TwisT) was shown and a realistic time, work, and budget estimate was given.

1 Introduction and Objectives

Within the scope of the already concluded R&D project GENESIS (Uhlig et al. 2007), DBE TECHNOLOGY GmbH developed repository reference models and designed underground mine layouts for the most promising clay formations and regions in Germany in such a way that the thermal boundary conditions were not exceeded. In addition to this, vertical movements (uplifts and subsidences) of the surface were calculated and first assessments regarding the mechanical stability of the drifts were made. Within the scope of design calculations, a disposal and barrier concept was developed that allows the emplacement of high-level, heat-generating waste in clay formations after tolerable interim storage times.

The concept is based on the emplacement of heat-generating waste in vertical boreholes with a depth of 50 m max. Depending on the waste container type, the boreholes are drilled at precisely defined distances to each other so that, even if there is a thermal influence between adjacent boreholes, the thermal boundary conditions of the buffer material are not exceeded. At the beginning, i.e. directly after emplacement, the temperature gradients in the near field of an emplacement borehole and in the geotechnical barrier are very high. Some chemical, hydraulic, and mechanical processes are highly temperature-dependent and may influence each other. For the assessment and demonstration of the repository safety, it is necessary to have adequate knowledge about the thermo-hydro-mechanical (THM) properties of the geotechnical barrier and to understand and be able to describe the coupled THM processes in the geotechnical barrier and the interactions between buffer and host rock that are due to the thermal interaction between adjacent emplacement boreholes.

In Germany, these thermo-hydro-mechanical interaction effects have been studied within the scope of the design calculations for a final repository in clay formations mentioned above, but only based on numerical calculations. The primary objective of previous in-situ heater experiments both at the laboratory in Mont Terri, Switzerland, (Opalinus clay) and at the underground research laboratory in Bure, France, (Callovo-Oxfordian clay) was to identify thermo-hydro-mechanical rock parameters and/or to study the sealing properties of a geotechnical bentonite barrier when heated (Rothfuchs et al. 2005), (GRS 2004). How strongly thermally induced interaction between adjacent emplacement boreholes affects a system of vertical boreholes in claystone has not yet been investigated in situ. However, these interaction effects are real as in a real repository the emplacement boreholes are drilled successively and, depending on the delivery and necessary cooling-off time of the containers at the interim storage facility, are filled at corresponding intervals.

The main issues in this context are (i) if and to what extent the permeability of the host rock changes over time due to the THM interactions, (ii) if and to what extent these interactions in the boreholes have a mechanical impact on the containers, and (iii) if thermally-induced cracks evolve in the host rock (mainly EDZ) which are subsequently either re-closed by the interaction effects or spread even further.

The planned twin-borehole heater experiment will address these and other issues and will thus not only significantly advance the understanding of the processes that take place due to this thermally induced interaction but also provide fundamental scientific and technical pa-

parameters for both the design of a specific repository and a well-founded long-term safety analysis of a repository in a clay formation in Germany.

The project is to be planned and carried out jointly by DBE TECHNOLOGY GmbH and GRS (en: Association for Plant and Reactor Safety). The Federal Institute for Geosciences and Natural Resources (BGR) has declared its interest in participating. However, a final decision can only be made after the reorganisation of BGR is completed and they know the resources they have available for a participation in the project. The project has met the interest of other members of the Mont Terri consortium as well, and there has been a positive vote to carry out the experiment at the Mont Terri laboratory.

The time and costs involved in such a major project cannot be reliably estimated without sufficient information. Thus, this feasibility study was carried out to establish a solid basis for the planning and implementation of the project.

2 Experimental Setup

2.1 Objectives of the TwisT Experiment

The main objective of the TwisT experiment is to test in situ and under representative thermal conditions the disposal and barrier concept which was developed in previous projects and to validate the design calculations. According to the design of the experiment, it is planned to equip two vertical boreholes with two canister dummies (electric heaters) each and to seal them in the way anticipated in the barrier concept. The experimental setup is to be equipped with sufficient sensors to monitor the THM interactions between both boreholes in the geotechnical barrier and in the host rock, and to obtain the data necessary to analyse the experiment by means of accompanying numerical calculations. One problem in earlier heater experiments was that often there were not enough temperature data from monitoring points. An insufficient number of temperature readings due to inconclusive results from several sensors and a series of malfunctions made a precise identification of parameters, especially regarding statistical analyses or inverse modelling, very difficult and led to equivocal results (Jobmann 2008).

Thus, one of the sub-goals of this experiment is to create a monitoring grid that is sufficiently detailed to allow the monitoring of the three-dimensional temperature development in the vicinity of the heaters. This is to provide the means to measure, visualise, and analyse by means of model calculations the heat propagation which, due to the layered structure of the Opalinus clay, is anisotropic. The closely spaced arrangement of the sensors is to allow the identification of local heterogeneities by means of a detailed parameter identification and perhaps adjustment of the constitutive law, respectively.

A further sub-goal of the in-situ experiment is to demonstrate the suitability of the phased closure concept. The phasing of the experiment is to be as close to reality as possible, i.e., the boreholes will be filled and heated with a corresponding delay. Realistic impacts on existing, unfilled boreholes will be identified making it possible to draw conclusions about probable borehole deformations, the borehole stability and, if applicable, about the corresponding minimum and maximum times the boreholes can remain open. After the heating of the second borehole, it is intended to determine the container loads in an already filled borehole.

For a safety demonstration it is necessary to characterise the excavation damaged zone (EDZ) as it is a potential migration pathway due to its increased permeability compared to intact host rock and barrier. A further issue of the experiment will be the characterisation of the evolution of the EDZ in an open borehole when a thermal load is applied via an adjacent borehole. It needs to be determined how the excavation damaged zone evolves under thermo-mechanical load.

Not only the excavation damaged zone but the host rock as well may be affected by the THM interactions. It is important to investigate if there is an induced crack generation and a corresponding increase in permeability.

A further aim of the project is to qualify the enhanced sealing effects of a clay-sand buffer at increased temperature under representative in-situ conditions. The work is considered to be a continuation and expansion of an R&D programme carried out at ambient temperature by GRS within the scope of their SB project ("Selfsealing Barriers of Clay/Sand Mixtures") and is to prove the suitability of the material as a buffer in emplacement boreholes for heat-generating waste in clay formations. The results for the clay-sand mixture are to be compared with the results for the bentonite-graphite mixture developed by DBE TECHNOLOGY GmbH. When adding graphite, the heat is adequately dissipated.

2.2 Location of the Twist Experiment

The experiment is to take place at the underground research laboratory (URL) in Mont Terri, Switzerland. At this location, the Opalinus clay is present as a sandy facies, among others, (area around niche 4, Figure 2-1). The sandy clay facies is also characteristic for the clay of the German part of the Molasse basin that may be taken into consideration in an extended site selection process as it was identified as a potentially suitable host rock in the BGR clay study (Hoth et al. 2007). The results of the experiment may more reliably applied to the German Molasse basin if the experiment is located in the sandy facies of the URL. Figure 2-1 shows the layout of the Mont Terri laboratory as of November 17, 2008, and the intended location of the experiment.

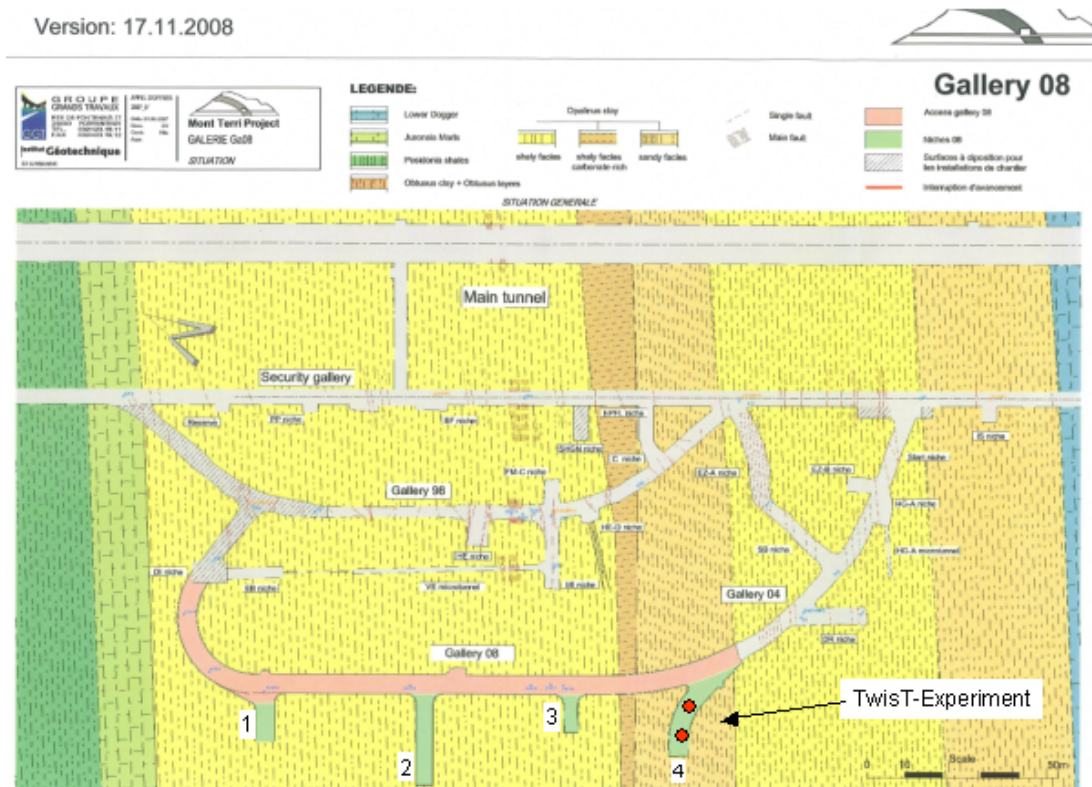


Figure 2-1: Layout of the underground research laboratory in Mont Terri as of November 17, 2008

2.3 Conceptual Design

The TwisT experiment comprises the installation of electric heaters in two adjacent vertical boreholes in a drift, simulating the heat generation of high-level waste to monitor the temperature impact on the host rock properties. The heaters will be constructed with a geometry similar to the German HAW casks having a cylindrical shape with a diameter of 0.43 m and a height of 1.30 m. The bentonite buffers around both heaters are planned to have a thickness of 0.40 m each. Thus, the necessary diameter of the heater boreholes will be about 1.30 m.

The two boreholes will be drilled within the same period of time. Subsequently, the first borehole will be equipped with a heater 1 and a bentonite-graphite buffer and the heating process will be started. The second borehole will stay open. After one year, the second borehole will be equipped with another heater, this time covered by a bentonite-sand buffer, and the second heater will be switched on. Both heaters will then be in operation for at least another year.

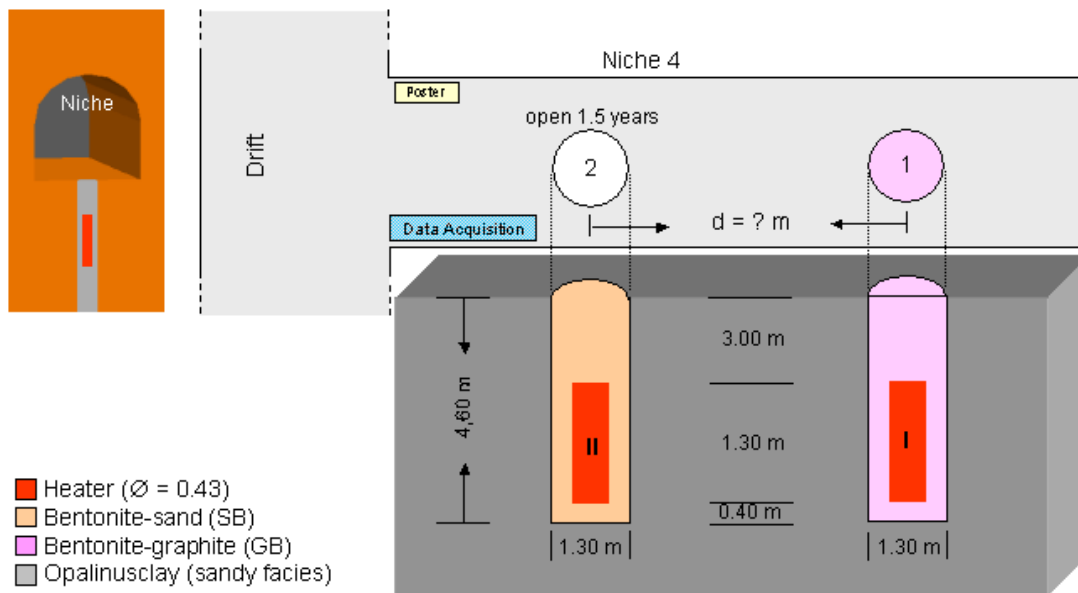


Figure 2-2: TwisT – conceptual design (not to scale)

For the design of **TwisT** including the monitoring system, calculations with regard to the development of temperature, deformation, and pore pressure resulting from heating are carried out, pursuing the optimisation of the thermal, mechanical and hydro-mechanical layout and providing information concerning the optimal sensor position and expected magnitudes of the measurands.

With regard to the **thermal design**, the following questions arise:

- Heater power: what is the required maximum heater power to achieve a temperature of 100°C¹ at the contacts bentonite/heater at both heaters ?
- Experiment Duration: what time is needed to reach a quasi-steady state of temperature between the heaters ?
- Borehole distance: at which distance is the thermal influence (temperature increase at borehole 2 while the heater 1 is in operation) less than the admissible temperature increase of 2 – 4 K, which corresponds to the repository design calculations in the framework of the development of the German reference disposal concept for argillaceous media ?

Regarding the **mechanical design**, the relevant questions are:

- what is the expected deformation and borehole convergence (especially for the open borehole 2) ?
- EDZ around borehole:
 - o extension and failure mode ?
 - o evolution with time (TM & HM load) ?
-> Experiment duration ?
- Borehole depth and distance (from mechanical point of view / borehole stability) ?

Regarding the **hydro-mechanical design**, the aim of modelling is to clarify the following questions:

- Expected maximum pore pressure ?
- Influence / disturbance due to drift drainage ?
- Influence / disturbance of pore pressure field due to EDZ ?
- Experiment duration / evolution of pore pressure ?
- Borehole depth and distance (from hydraulic point of view)?

¹ At temperatures exceeding 100 °C a release of crystal water most likely occurs, which results in a change of the favourable properties of the bentonite (i.e. high sorption capacity, low permeability).

3 Design Calculations

3.1 Continuum Model

3.1.1 Geometry

A general view and the dimensions of the established model are shown in Figure 3-1. The model comprises a volume of rock containing a horseshoe-shaped drift of 4.5 m in width, 4.6 m in height and 15 m in length, which is cut in half. Due to the symmetry boundary conditions (horizontal bedding of the Opalinus clay, adiabatic boundaries), the model represents one-fourth of borehole 1 and heater 1 and one-half of borehole 2 and heater 2 (Figure 3-2).

The borehole diameter is 1.05 m and the length is 4.6 m, the heater has a diameter of 0.43 m and is 1.3 m in height. According to the disposal concept (Jobmann et al. 2007), the space between the heater and the Opalinus clay is filled with bentonite. The borehole is blanked off with a bentonite plug which is 3 m in height measured from the top of the heater to the drift floor (Figure 2-2). The borehole bottom consists of a 0.3-m thick bentonite bed.

The borehole-to-borehole distance was the only parameter varied within the model geometry. In the first model layout, a borehole distance of 8 m was used, which was reduced to 6 m in the course of the calculations. Figure 3-1 shows the model mainly used in which the borehole distance is 6 m. It consists of 38,935 zones and contains 42,377 gridpoints. A refined model discretisation is used in the vicinity of the boreholes and the zone size varies from $1.58 \cdot 10^{-3}$ to 15.59 m^3 .

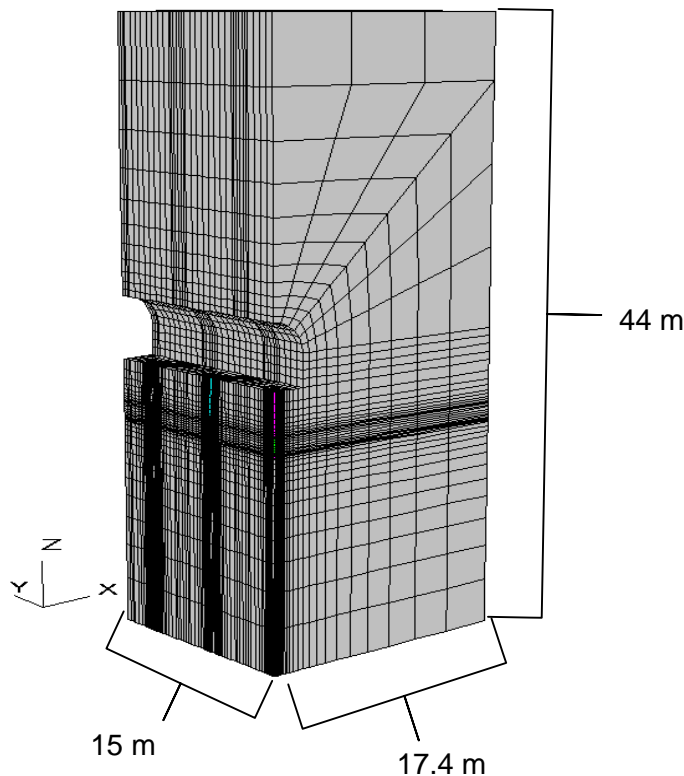


Figure 3-1: Numerical model used for THM calculations – model dimensions

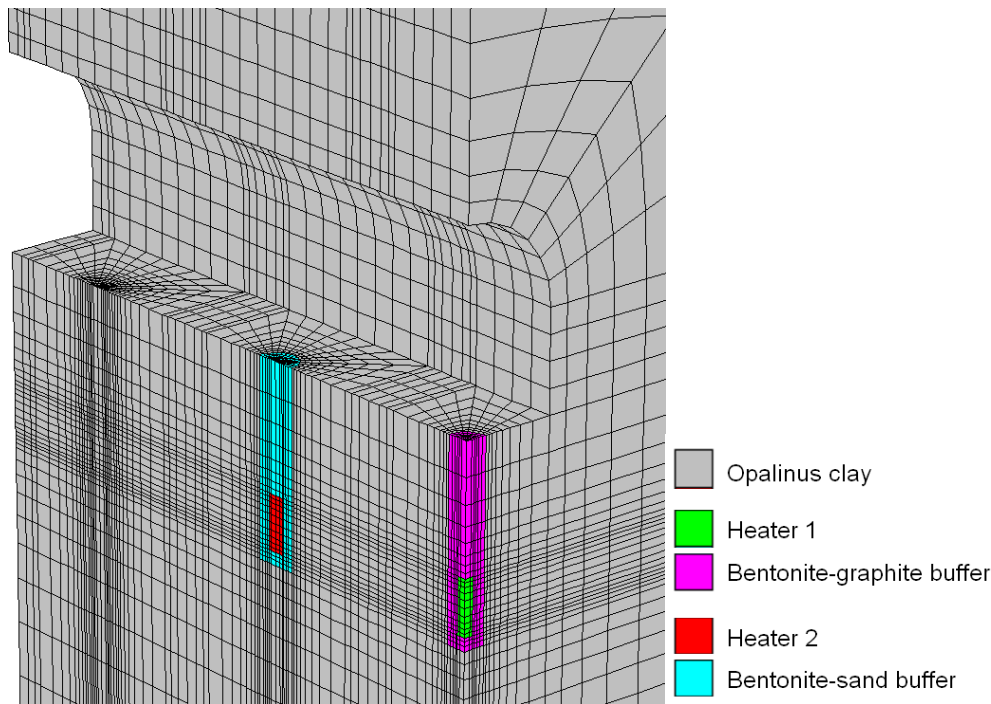


Figure 3-2: Numerical model used for the THM calculations – boreholes and heaters, implemented materials

3.1.2 Constitutive Models

The model employed considers Opalinus clay as host rock and boreholes which enclose the heaters and buffer material (cf. Figure 3-2). In the first borehole, a bentonite-graphite buffer is used which has a higher heat conductivity than the bentonite-sand buffer which is filled in borehole 2.

In order to simulate the behaviour of the Opalinus clay and the bentonite buffer, a coupled thermal-hydraulic-mechanical modelling is carried out: The heaters are considered to be impermeable, hence, only a thermal-mechanical model is applied.

Opalinus clay

The **mechanical behaviour** of the host rock was modelled as an elasto-plastic model and alternatively - in one model layout – a creep model is used, which describes rheologic behaviour of the host rock.

Elasto-plastic material model

The elasto-plastic material model (Mohr-Coulomb) used within this investigation takes into account:

- anisotropic strength behaviour distinguishing matrix- and/or bedding failure due to shear and/or tension,
- strain hardening before failure (reduction of elastic parameters),
- strain softening after failure (reduction of matrix and/or joint strength).

Creep model

The creep of the Opalinus clay is modelled through a constitutive law which combines the visco-elastic Norton Power Law and the Mohr-Coulomb elasto-plastic model. In a first approach the Norton Power Law considers only the stationary creep phase. The creep rate is:

$$\dot{\varepsilon} = A \cdot \sigma^n \quad (6-5)$$

- A power law constant
- n power law exponent, $n = 1$
- σ von Mises stress

The mechanical model was coupled to a **hydraulic model** which considered the Opalinus clay as a porous medium. The flow is described by a single-phase fluid flow after Darcy's law. The following assumptions were made:

- full initial saturation,
- isotropic hydraulic properties,
- increase of k_f by a factor of 10 after rock mass failure (applies particularly to the excavation damaged zone).

Furthermore, a **thermal model** based on the energy conservation and Fourier's Law for heat transport was implemented. The heat transport is assumed to be anisotropic.

Buffer

For modelling the mechanical behaviour of the bentonite buffers, an elasto-plastic constitutive law (Mohr-Coulomb) for a frictionless hardening material is used which assumes that after a state of plasticity has been reached, the cohesion increases with accumulated plastic shear strain. For the flow a single-phase fluid flow after Darcy's law is applied considering an initial saturation of 80%. The hydraulic properties are assumed to be isotropic. The heat transport is modelled as an isotropic process using Fourier's Law.

Heaters

The heaters are assumed to constitute a simple elastic, isotropic material with linear stress-strain behaviour with no hysteresis on unloading. The heaters are assumed to be impermeable, therefore no flow model was applied. The heat transport is modelled as an isotropic process using Fourier's Law.

3.1.3 Model Parameters

3.1.3.1 Thermal, hydraulic, and mechanical parameters

Table 3-1: Thermal, hydraulic, and mechanical model parameter

		Opalinus Clay (sandy facies)		Bentonite- graphite	Bentonite- sand	Heater	Air
		matrix	bedding				
Thermal parameters							
Density ρ	[kg/m ³]	2 450 ^{/1/}		2 000	2 000	4 000 *	1.12
Thermal conductivity λ	[W/(m·K)]	\perp 2.76 ^{/1/} \parallel 1.31 ^{/1/} anisotropy 2,1 ^{/1/}		2.5	1.35	5.0 *	0.0257
Specific heat capacity c_p	[W/(kg·K)]	920 ^{/2/}		800	1 000	1 000 *	1 007
Thermal expansion	[K ⁻¹]	2.4e-5		2.5e-5	2.5e-5	1.e-5	
Hydraulic parameters							
Hydraulic conductivity k_f	[m/s]	\perp \parallel 5e ⁻¹³ ^{/1/} variation: 5e-12 *		1e ⁻¹⁴ *		0.0	
Porosity n	[%]	13.5 ^{/1/}		40 *			
Biot modulus M	[MPa]	8 000 ^{/1/}		2 000 *			
Biot coefficient b	[-]	0.6 ^{/1/}		0.8 *			
Mechanical parameters							
Behaviour		Elasto-plastic strain softening		Elasto-plastic hardening	Elastic		
Young's modulus E	[MPa]	7 000		5 000	10 000		
Poisson ratio ν	[-]	0.27		0.4	0.2		
Pre-failure behaviour (Opalinus clay failure strain 1 %)							
Angle of friction Φ	[°]	30	34	0			
Cohesion c	[MPa]	8.7	1.3	4.3 (increasing with ϵ_p)			
Tensile strength R_t	[MPa]	2.5	1.2				
Dilation angle Ψ	[-]	0	0				
Post-failure behaviour (Opalinus clay failure strain 1 %)							
Angle of friction Φ	[°]	29	33	0			
Cohesion c	[MPa]	4.3	0.7	15 (at $\epsilon_p \geq 1.8$ %)			
Tensile strength R_t	[MPa]	0.01	0.01	0.01			
Dilation angle Ψ	[-]	0	0	0			
Parameter set with reduced strength properties for failure and post-failure							
Pre-failure behaviour (Opalinus clay failure strain 1 %)							
Angle of friction Φ	[°]	25	23	0			
Cohesion c	[MPa]	2.2	1.0	4.3 (increasing with ϵ_p)			
Tensile strength R_t	[MPa]	1.0 ^{/2/}	0.5 ^{/2/}				
Dilation angle Ψ	[-]	0	0				
Post-failure behaviour (Opalinus clay failure strain 1 %)							
Angle of friction Φ	[°]	25 *	23 *	0			
Cohesion c	[MPa]	1.1 *	0.5 *	15 (at $\epsilon_p \geq 1.8$ %)			
Tensile strength R_t	[MPa]	0.001 *	0.001 *	0.01			
Dilation angle Ψ	[-]	0 *	0 *	0			

^{/1/}(ANDRA 2005) ^{/2/}(NAGRA 2002) * Assumption

3.1.3.2 Creep Model

The parameters implemented in the creep model correspond to results gained from creep experiments, where at a load of 5 MPa a stationary creep rate of $1e-11$ 1/s was observed which led to a power law constant A of $2.6e-11$ 1/s (GRS 2004).

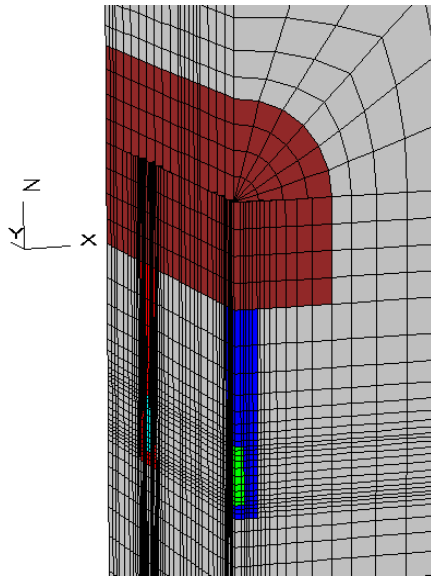
Time-dependent deformation tests of the Opalinus clay conducted by NAGRA (NAGRA NTB 02-03) have shown that at low deviatoric stresses the creep rate is zero and significant creep occurs at high deviatoric stress. Only after a lasting impact of a high load a stationary creep rate was observed. In order to take those results into account, a threshold value was introduced which represents the effective stress of the initial state (4.115 MPa). The creep parameter A is zero if the current stress state is below the threshold value, hence, creep occurs only when the current state exceeds 4.115 MPa.

Table 3-2: Creep parameters

	<i>Opalinus Clay (sandy facies)</i>		<i>Bentonite- graphite</i>	<i>Bentonite- sand</i>	<i>Heater</i>	<i>Air</i>
	<i>matrix</i>	<i>bedding</i>				
Mechanical parameters						
Behaviour	Creep		Elasto-plastic hardening		Elastic	
Young's modulus E [MPa]	7 000		5 000		10 000	
Poisson ratio ν [-]	0.27		0.4		0.2	
Angle of friction Φ [°]	30.0		0			
Cohesion c [MPa]	5.0		4.3 (increasing with ϵ_p)			
Tensile strength R_t [MPa]	2.0					
Dilation angle Ψ [-]	0					
Creep parameter						
Power Law Constant A [1/s]	2.6e-11					
Threshold value [MPa]	4.115					

3.1.4 Initial conditions

For the initial stress state the following conditions are assumed:



$$\begin{aligned} \sigma_v &= 6.5 \text{ MPa} && (z) \\ \sigma_H &= 4.3 \text{ MPa} && (y, \text{ along drift axis}) \\ \sigma_h &= 2.2 \text{ MPa} && (x, \text{ normal drift axis}) \end{aligned}$$

Initial temperature: $T = 15^\circ\text{C} = \text{const.}$

Figure 3-3: Initial stress state

The initial hydraulic conditions are the following:

Table 3-3: Initial hydraulic conditions

	Opalinus Clay	Buffer
Pore pressure [MPa]	2, gradient: 0.01 / m	0
Saturation [-]	1	0.8

3.1.5 Simulation Workflow

In the preliminary experiment design the following workflow is foreseen:

Table 3-4: Workflow of the model simulation

	Simulation time [d]	
autumn 2008	-486	drift excavation (instantaneous) drainage for ~15 month
winter 2009	-30	borehole drilling drainage 1 months
winter 2009	0	start heater 1
winter 2010	365	start heater 2
winter 2011	730	end of heating heat dissipation period, dismantling

3.1.6 Model Layouts

In order to obtain the optimal thermal layout the influence of two different thermal boundary conditions was investigated: (a) fixed temperature at the drift contour, (b) convection within the drift. Furthermore, the heater power and the distance between the boreholes were modified.

In order to analyse a range of possible hydro-mechanical results, three different mechanical model layouts were compared:

- elasto-plastic model distinguishing matrix and joint behaviour (reference model),
- elasto-plastic model distinguishing matrix and joint behaviour with reduced strength parameters,
- creep model, assuming homogeneous isotropic strength behaviour.

The thermal and hydraulic models remained the same.

3.2 Results

Generally, the results were obtained through a coupled thermal, hydraulic and mechanical modelling approach; the distance between the boreholes was 6 m, and the heater power was: P1: 968 W and P2: 711 W. Results obtained through application of a different borehole distance or heater power will be indicated. Figure 3-4 shows the position of the observation points at which the temperature and the pore pressure were recorded during the model simulation.

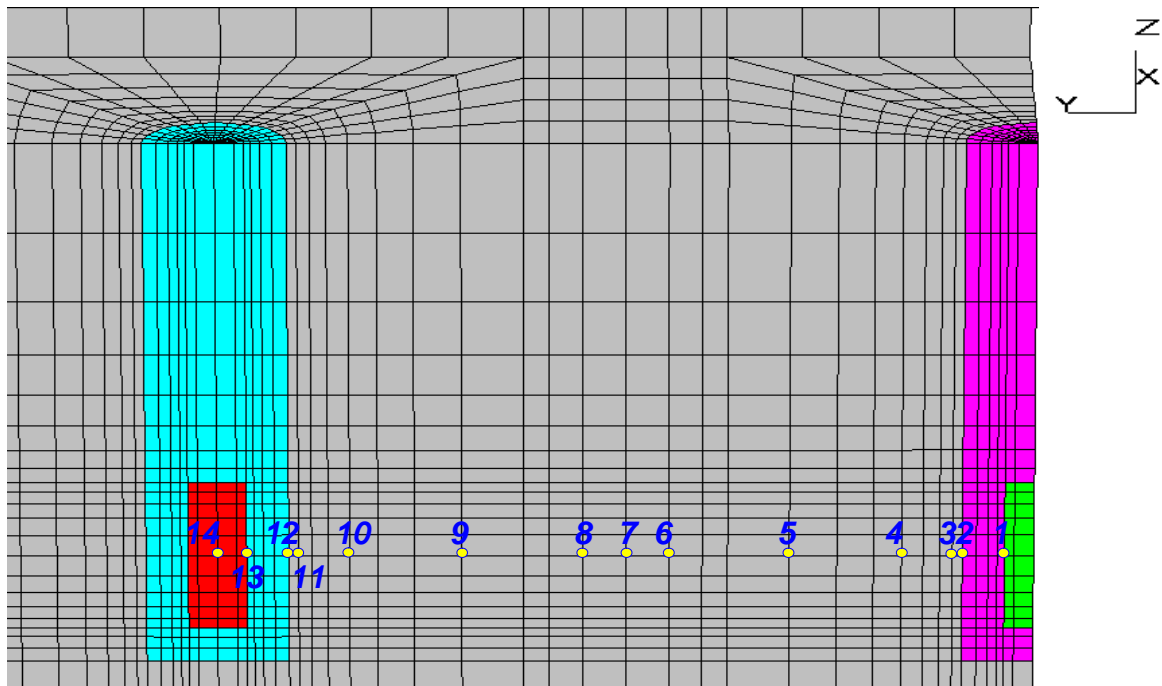


Figure 3-4: Observation points for temperature and pore pressure

Table 3-5: Position of the observation points

Observation point number	Distance to borehole 1 along y-axis [m]	Elevation [m]	Explanatory notes
1	0.22	-3.65	Interface heater 1/bentonite
2	0.53	-3.65	Interface bentonite/Opalinus clay
3	0.60	-3.65	Opalinus clay
4	0.97	-3.65	Opalinus clay
5	1.80	-3.65	Opalinus clay
6	2.68	-3.65	Opalinus clay
7	3.00	-3.65	Opalinus clay
8	3.32	-3.65	Opalinus clay
9	4.20	-3.65	Opalinus clay
10	5.03	-3.65	Opalinus clay
11	5.40	-3.65	Opalinus clay
12	5.48	-3.65	Interface bentonite/Opalinus clay
13	5.79	-3.65	Interface heater 2/bentonite
14	6.00	-3.65	Within heater 2

3.2.1 Thermal Layout

The heating process at borehole 1 starts at $t = 0$ d, whereas heater 2 is put into operation at $t = 365$ d. The objective is to reach 100 °C at the contacts heater/bentonite during the simulation. At the same time, an inadequate temperature increase at borehole 2 is to be avoided; the admissible temperature increase at borehole 2 due to heating at borehole 1 was defined to be $2 - 4\text{ K}$, which corresponds to repository design calculations.

One test layout was used to investigate the influence of two different thermal boundary conditions:

- (a) fixing the temperature at the drift contour at 15 °C ,
- (b) convection within the niche².

Figure 3-5 shows the thermally influenced zone at a specific heating time for a specific temperature increase. The radius of the thermally influenced zone decreases if the temperature within the drift is fixed, compared to the thermal model which considers convection due to air circulation in the drift (Figure 3-5). A fixed drift temperature results in a temperature of 15 °C at the contact host rock/drift. In the convection model, the temperature at the contact host rock/drift is governed by a gradient that depends on the temperature of the host rock which is affected by the heating, the air temperature in the drift (15 °C) and the heat transfer coefficient; presumably the temperature is higher than 15 °C , hence, less heat is dissipated.

² The heat transfer was estimated using the heat transfer coefficient α [$\text{W}/(\text{m}^2\cdot\text{K})$] : $q = \alpha \cdot A \cdot (T - T_0)$ with $q =$ heat flux [$\text{W}/(\text{J}\cdot\text{s})$], $A =$ surface area [m^2], $T - T_0 =$ temperature difference.

The red ellipse shows the range in which the temperature increase does not exceed the admissible change of temperature. The position of the red circle indicates that the admissible increase of temperature is met for a borehole distance of ca. 6 – 8 m.

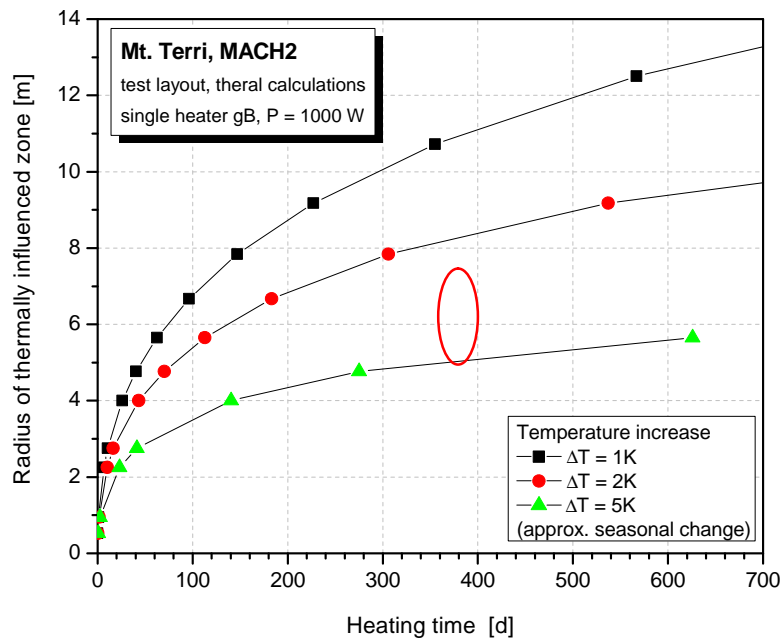


Figure 3-5: Impact of heating at heater 1 (P = 1000 W) and influence of convection

During further simulations, convection was not taken into account. Figure 3-6 shows the temperature for two different model geometries using a borehole-to-borehole distance of 6 m and 8 m, respectively; in the layout applying a borehole distance of 6 m, the temperature at the observation points is not significantly higher than in the layout with a borehole distance of 8 m. This is due to the fact that a reduced borehole distance increases the impact of superposition of the heat sources. Figure 3-6 shows that the increase of temperature caused by the initiation of the heating process at the opposite heater is more significant for the model layout with 6 m borehole distance than for the one with 8 m borehole distance. The temperature increase at borehole 2, while heating at borehole 1, is below the admissible increase of 4 –5 K for both model layouts. The subsequent model calculations were performed with the 6-m borehole distance. The applied heater power ($P_1 = 955.5 \text{ W}$, $P_2 = 637 \text{ W}$) proved to be insufficient for reaching a temperature of 100 °C at both contacts heater/buffer. Hence, the heater power had to be increased.

Figure 3-7 shows the temperature evolution at the contacts heater1/buffer (OP1) and heater2/buffer (OP13) for different heater powers. As the heat conductivity of the bentonite-graphite buffer is almost double the heat conductivity of the bentonite-sand buffer (cf. Table 3-1), a higher heater power is applied at borehole 1. The temperature increase at the interface bentonite/heater 2 while heating at borehole 1 is less than 3.32 K at any tested heater power (Figure 3-6).

A heater power of $P1 = 968$ and $P2 = 711$ W was used in subsequent simulations in order to achieve a temperature close to $100\text{ }^{\circ}\text{C}$.

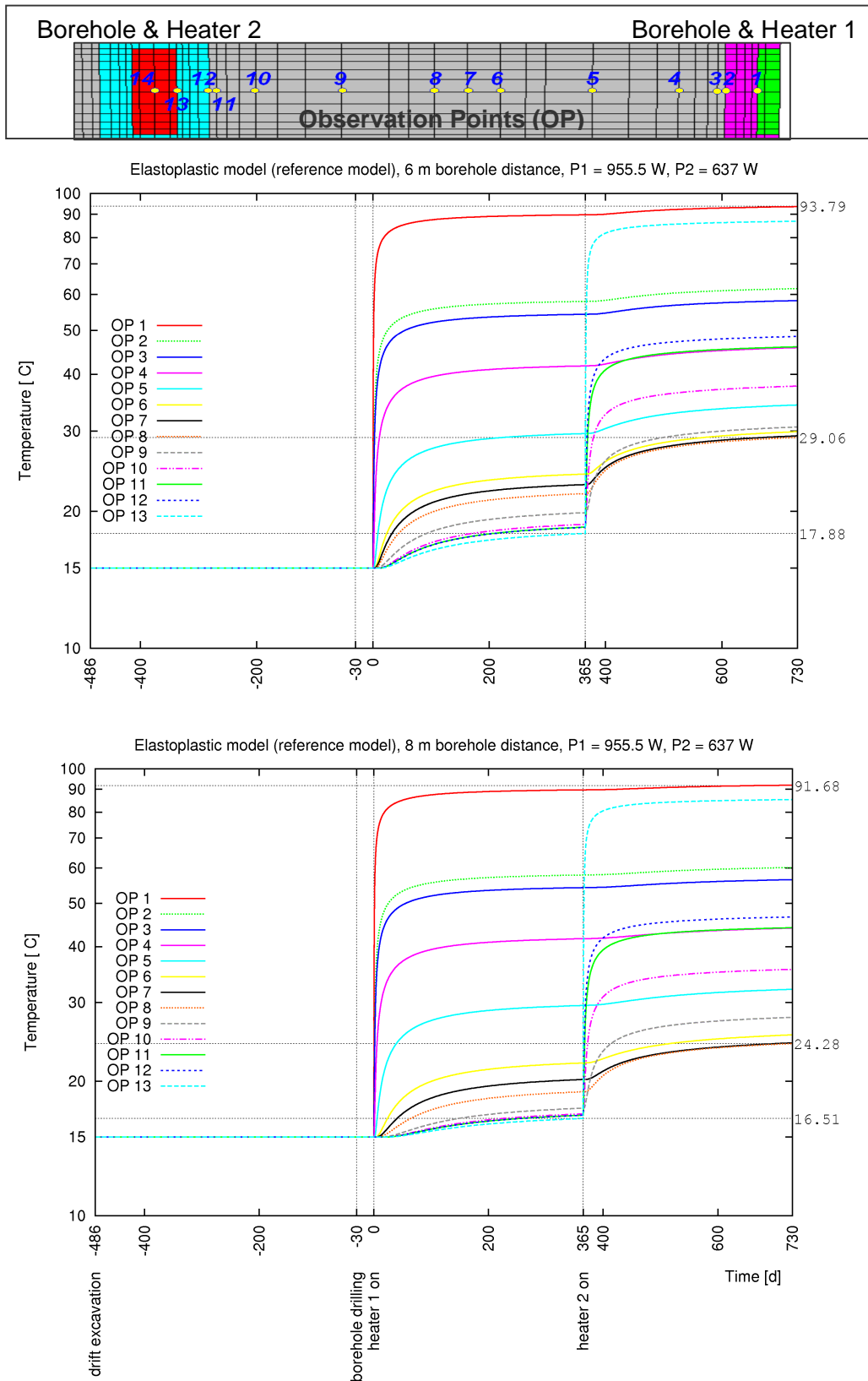


Figure 3-6: Comparison of the temperature evolution at the observation points for model layouts applying a borehole distance of 6 m and 8 m, respectively

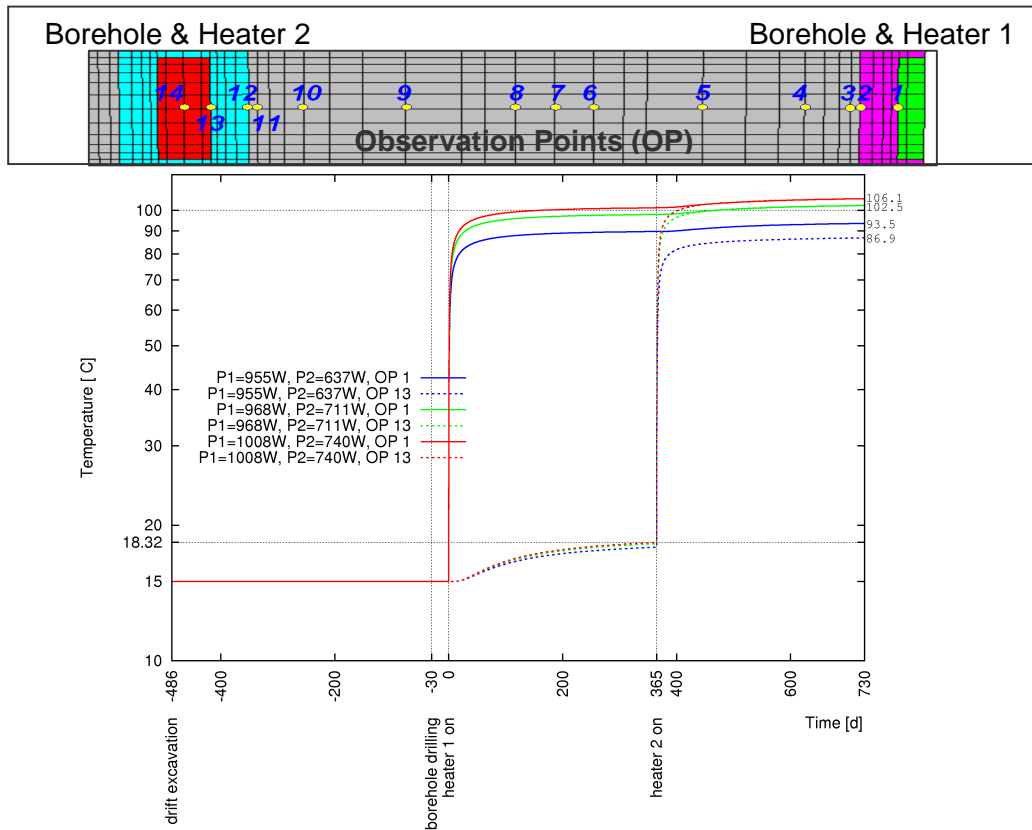


Figure 3-7: Temperature at the contact heater/bentonite for different heater powers

Figure 3-8 shows the temperature evolution at the observation points with P1 = 968 W and P2 = 711 W. The temperature increase caused by heating decreases when the distance to the heater in operation is increased. Nevertheless, at all observation points the initiation of the heating process at both heaters can be identified.

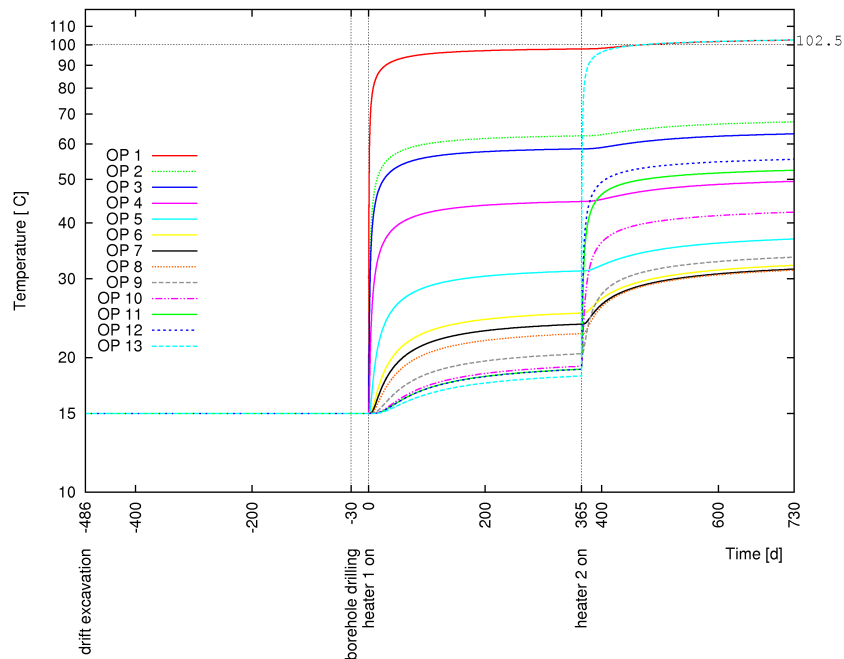


Figure 3-8: Temperature at all observation points, P1 = 968 W, P2 = 711 W

The top of Figure 3-9 shows the temperature field after operation of a single heater for a period of 365 days, when the second heater is taken into operation and the simultaneous heating process begins. In borehole 2, containing the bentonite-sand buffer, a lower heater power was assigned. The simultaneous heating for another year resulted in the temperature field shown at the bottom of Figure 3-9.

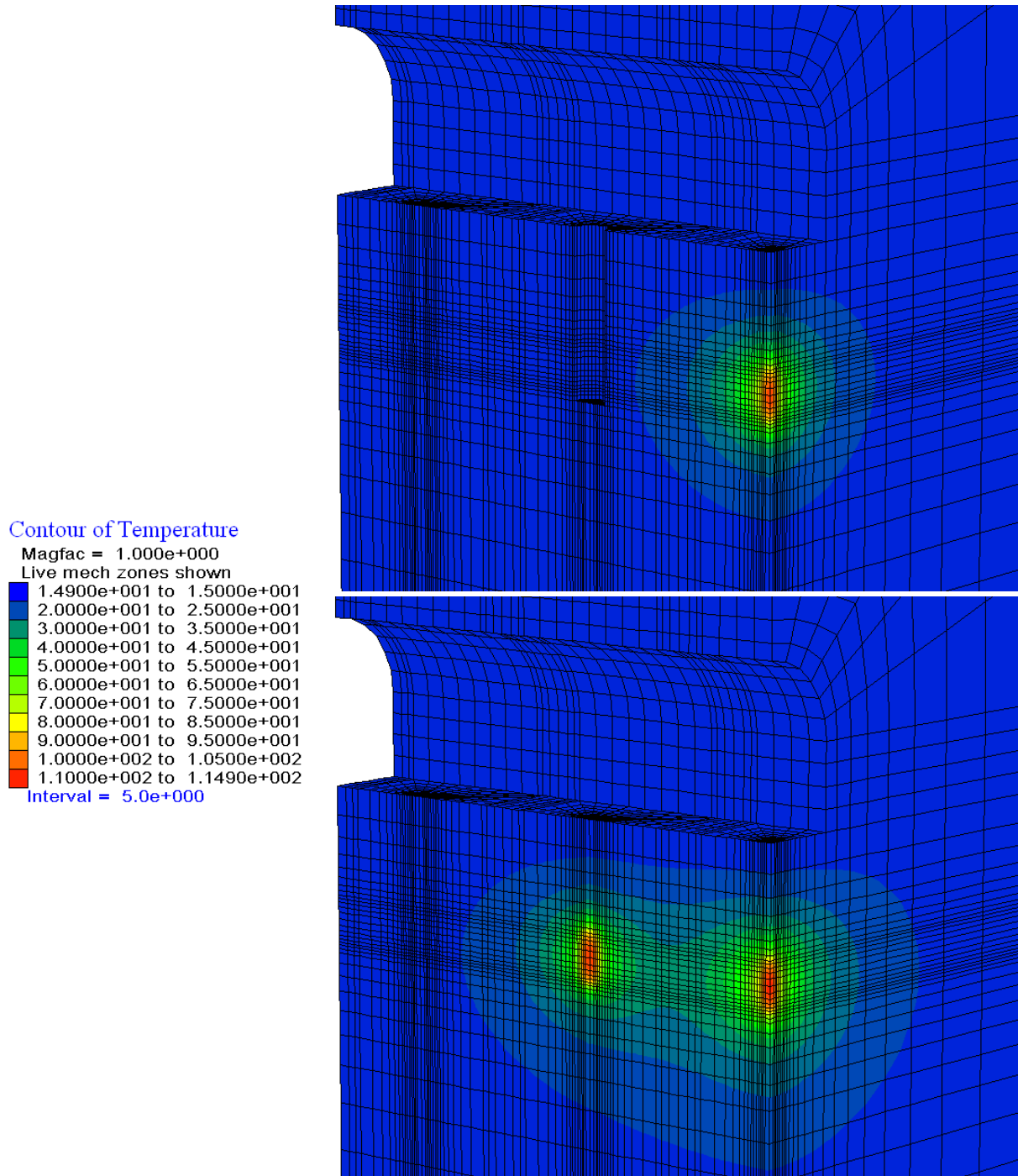


Figure 3-9: Temperature field after 365 days (top) and after 730 days (bottom) at $P1 = 968 \text{ W}$ and $P2 = 711 \text{ W}$

3.2.2 Hydro-mechanical Layout

3.2.2.1 Pore Pressure

The initial pore pressure is about 1.8 – 2.2 MPa with a vertical gradient of 0.01 MPa/m, thus, it increases linearly over depth, as is shown on the left hand side of Figure 3-10. Due to excavation, the pore pressure close to the drift decreases to below 1 MPa, in the drift floor and drift roof the pore pressure decreases to zero, and ~ 2 m behind the drift wall the pore pressure reaches a maximum value of ~3 MPa due to stress redistribution after excavation (right hand side of Figure 3-10). Figure 3-11 shows the predicted pore pressure after 486 days of drainage. The maximum pore pressure has decreased to its initial state, and the pressure field is characterised by a decreasing pore pressure towards the drift and the boreholes. Accordingly, the flow is directed towards the drift and towards the boreholes, respectively (see right hand side of Figure 3-11).

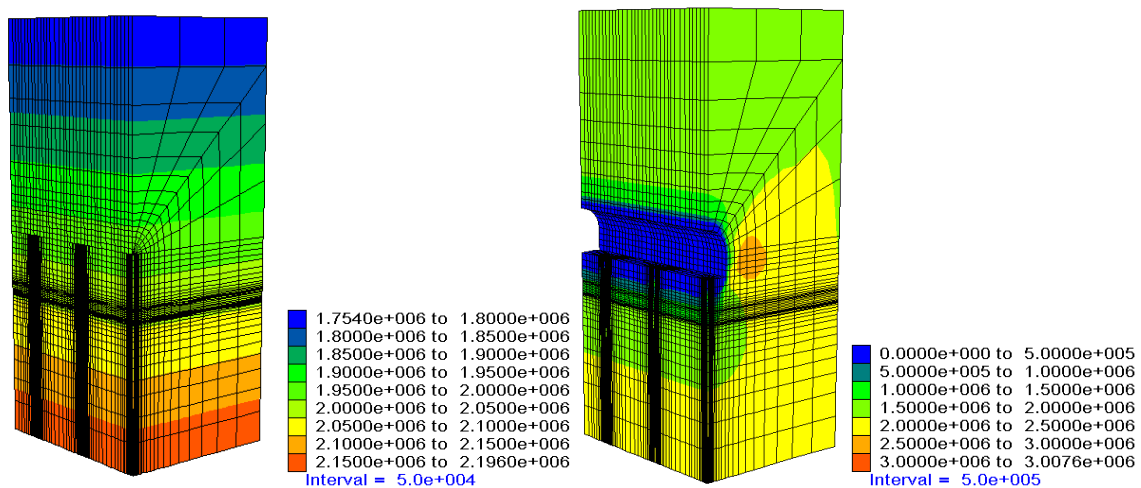


Figure 3-10: Pore pressure at the hydromechanical equilibrium before (left) and immediately after drift excavation (right)

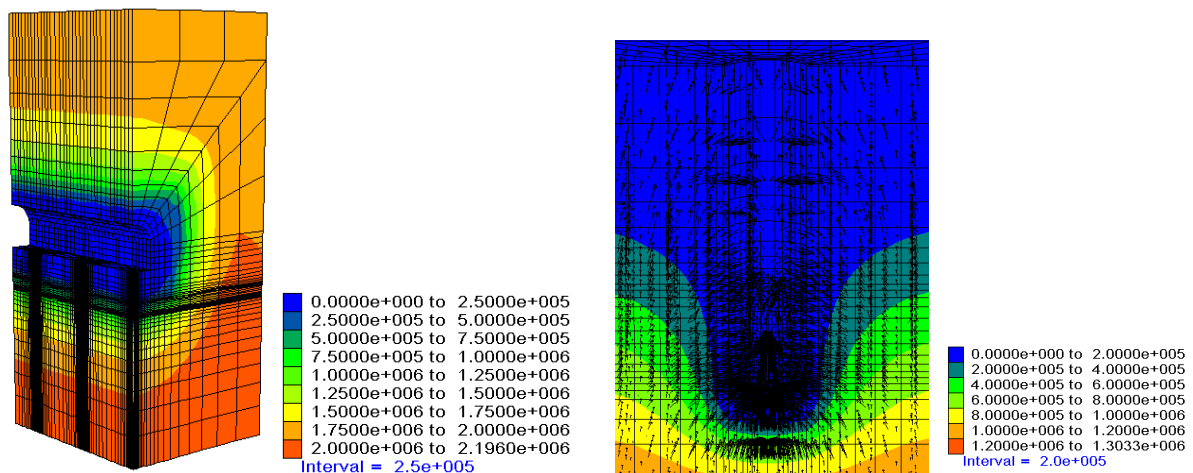


Figure 3-11: Pore pressure before heating at t = 0d: pore pressure field (left) and flow direction at borehole 2 (right)

The increase in temperature results in the expansion of the host rock and the fluid. This expansion cannot be evened out because the heat expansion occurs faster compared to the flow velocity of the fluid, which is very low due to the low permeability of the Opalinus clay. Therefore, thermally induced pore pressure increase is generated which increases with the heater power.

With respect to the mechanical layout, three different models were compared (cf. chapter 3.1.6). In the elasto-plastic model with reduced strength properties, the pore pressure at all time stages is lower than in the reference model, because for reduced strength properties the failure state is reached at lower loads. In the failure state, the volumetric deformation (extension) increases which results in a reduction of pore pressure. In the creep model, the rheologic behaviour of the Opalinus clay results in stress redistributions and volumetric compression so that the pore pressure is higher than in the reference model (creep model), (see Figure 3-13 - Figure 3-15).

Figure 3-12 shows the evolution of the pore pressure for the three different model layouts. The pore pressure field at $t = 0$ d shows the influence of excavation and borehole drilling depending on the mechanical model. The Opalinus clay close to the drift and close to the boreholes is drained, therefore, the pore pressure at the borehole and drift contour decreases. The pressure field at $t = 0$ d indicates that the most intensive drainage occurs in the elasto-plastic model with reduced strength, whereas the creep model exhibits the lowest drainage.

In all three model layouts, the highest pore pressure of the entire simulation is observed after approximately 30 days of heating close to heater 1 due to thermal expansion induced by the heating. The reference and the creep model show maximum values of ~ 3.0 and ~ 3.1 MPa, respectively. The maximum pore pressure of the model with reduced strength parameters is lower (~ 2.7 MPa) due to volumetric expansion of plasticized zones and an increased permeability of these zones (by a factor of 10). Afterwards, the pore pressure dissipates through drainage towards the drift and surrounding host rock so that the pore pressure maximum is reduced.

After approximately $t = 395$ d, the second pore pressure maximum occurs close to borehole 2, caused by heating at borehole 2 which starts at $t = 365$ d. This pore pressure maximum is lower than the pore pressure maximum at $t = 30$ d (reference model: ~ 2.5 MPa, elasto-plastic model with reduced strength: ~ 2.1 MPa, creep model: ~ 2.6 MPa, compare Figure 3-13 - Figure 3-15), since borehole 2 had already been drained for one year when it was left open, and the lower heat conductivity of the bentonite/sand buffer causes a slower heat propagation. Additionally, the applied heater power is lower compared to heater 1. The pore pressure maximum at borehole 2 is subsequently relieved and a rather layered pore pressure field develops slowly according to the pressure gradient.

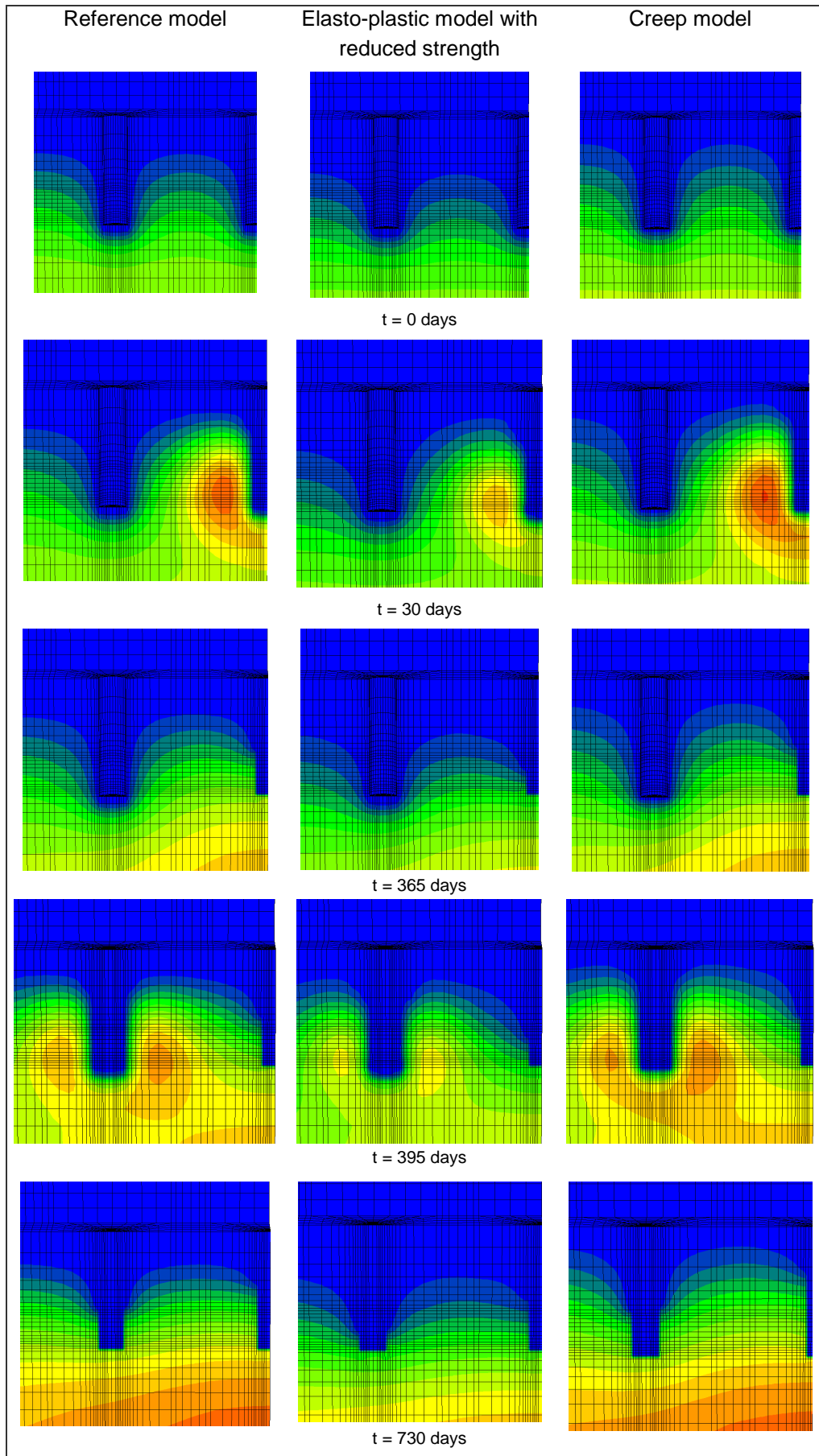


Figure 3-12: Evolution of the pore pressure field for the different model layouts

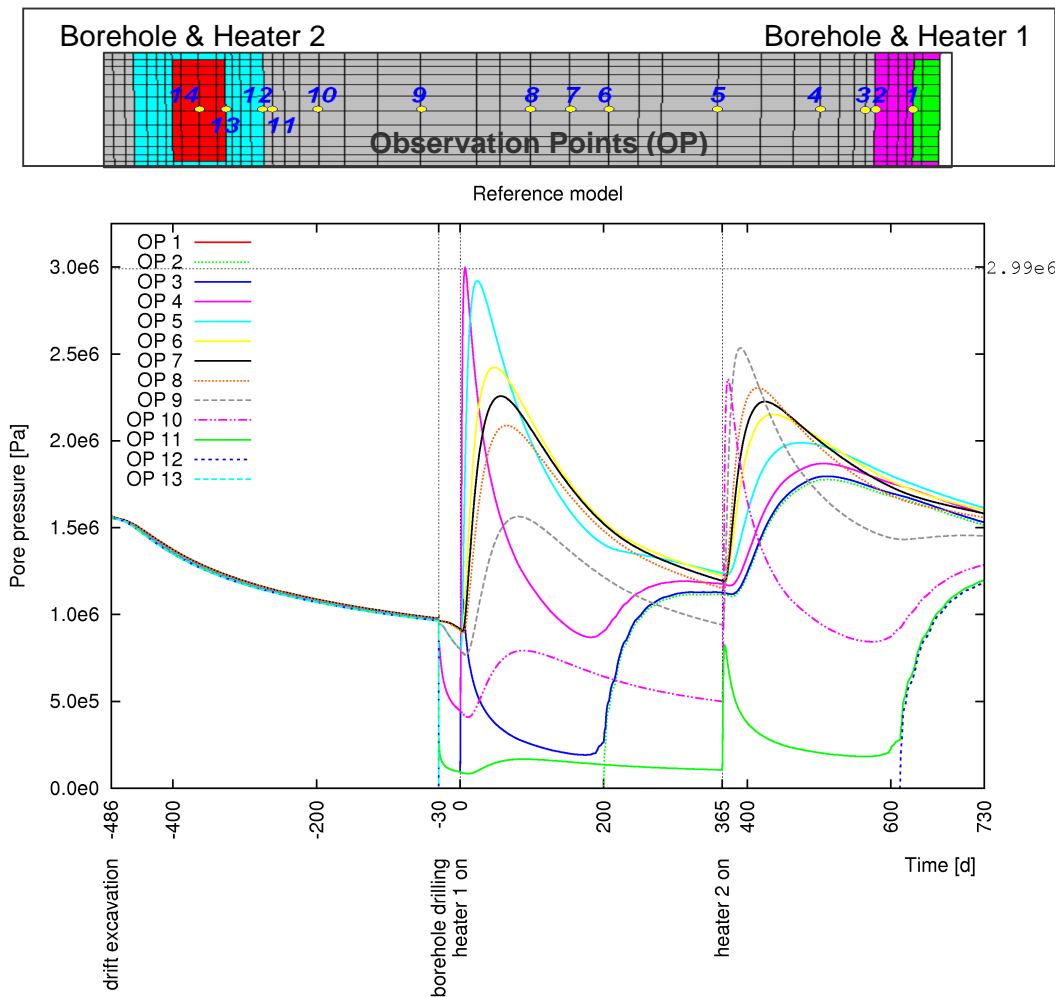


Figure 3-13: Pore pressure at the observation points, reference model

The pore pressure around the boreholes drops down to zero after excavation. The pore pressure at the observation points OP1 and OP 13, which are located at the contacts buffer/heater, decreases to zero after borehole drilling and the pressure remains low (Figure 3-13 - Figure 3-15). The pore pressure at the contacts buffer/host rock also decreases to zero at first. After the heaters and the buffers are installed in the borehole, the pore pressure slowly increases in the vicinity of the borehole and within the buffer. At the contact buffer/host rock the pore pressure increases only after some heating time at the respective heater, which is ~200 days at borehole 1 (OP 2, t = 200 d), and ~245 days at borehole 2 (OP 12, t = 605 d).

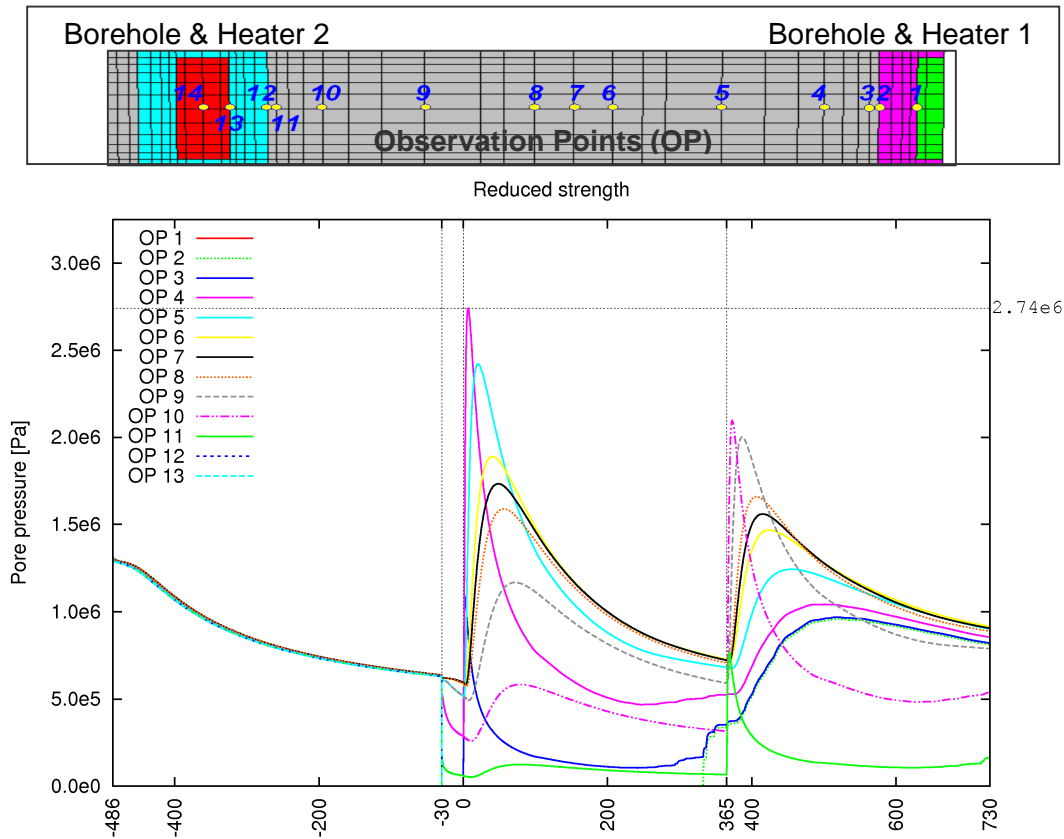


Figure 3-14: Pore pressure at the observation points, elasto-plastic model with reduced strength properties

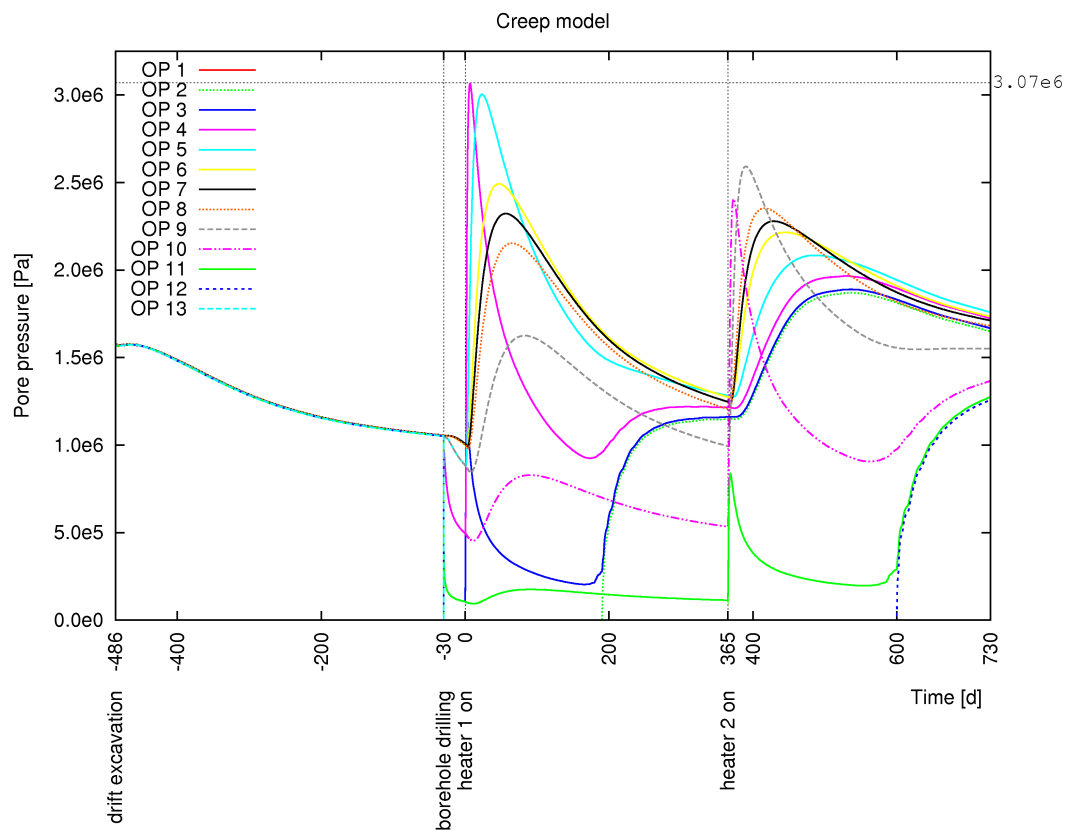
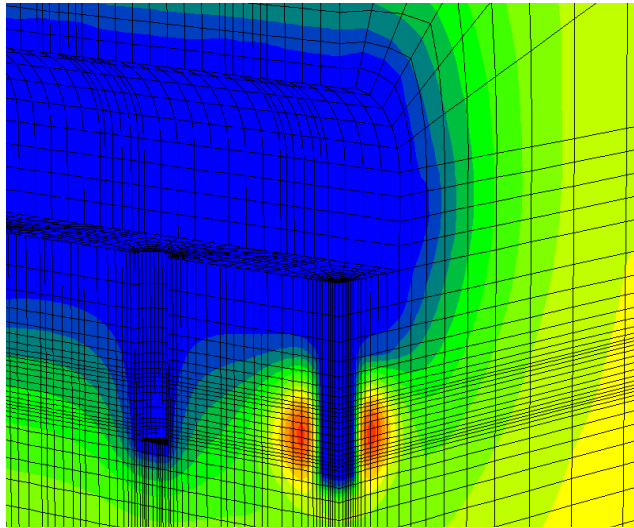
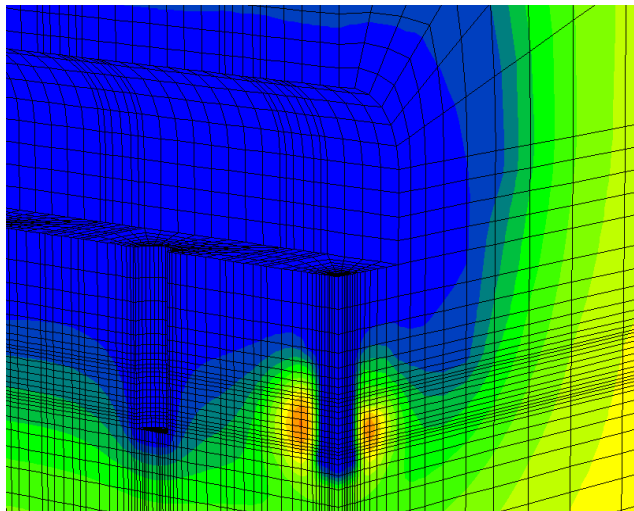


Figure 3-15: Pore pressure at the observation points, creep model

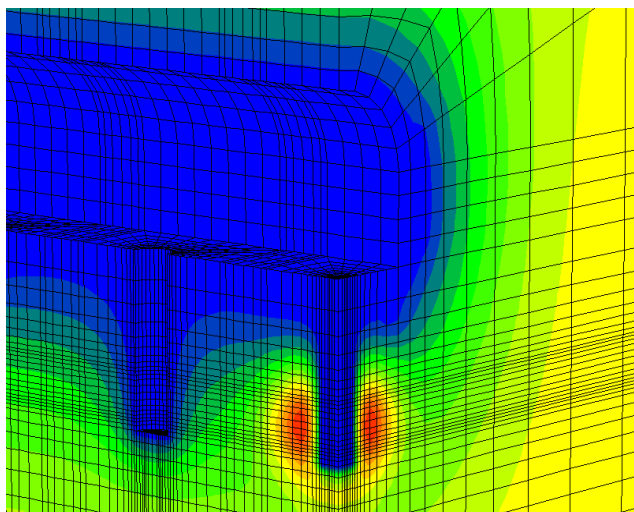
Figure 3-16 shows the drainage zone surrounding the drift and the boreholes as well as the pore pressure maximum at borehole 1 after 10 days of heating. At the drift walls, the pore pressure is zero. In the reference model and the creep model, the drainage is less pronounced than in the elasto-plastic model with reduced strength properties.



reference model



elasto-plastic model with reduced strength



creep model

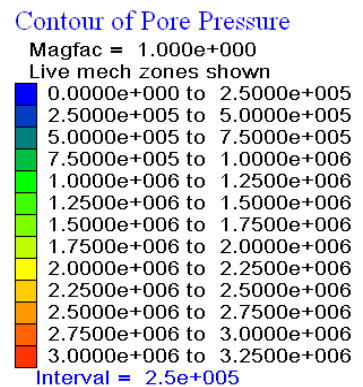


Figure 3-16: Pore pressure field after 10 days of heating at heater 1, approximately at this point of time the maximum pore pressure occurs in the simulation

3.2.2.2 States of Stress and Failure

In order to evaluate the state of stress the ratio between the actual stress and the rock mass strength can be calculated which gives values between 0 and 1. A stress/strength ratio of 1 implies that the yield state is reached. At a stress/strength ratio of 0.5 half of the load capacity is reached. Figure 3-17 and Figure 3-18 show the stress/strength ratio at $t = 365$ days and $t = 730$ days.

After one year of heating at heater 1 failure occurs in the drift floor, drift roof and in a small band within the drift walls in both, the reference model and the creep model (Figure 3-17), which indicates an excavation damaged zone (EDZ). The extent of the EDZ is ~ 0.75 m in the drift floor and ~ 0.45 m in the drift roof and walls. In the elasto-plastic model using reduced strength properties, the failure region comprises the entire drift contour, and the failure zone extends to up to ~ 2 m behind the drift wall (centre of Figure 3-17). Figure 3-17 shows that the load ratio in the host rock close to the first heater is higher than the stress/strength ratio in the host rock surrounding borehole 2 (at this time heater 2 was not yet in operation).

It has to be noted that the numerical mesh used for the simulations was not adopted to investigate the initiation and propagation of the EDZ surrounding the drift; since the discretisation close to the drift is quite coarse, the interpretation of the model results with respect to the EDZ may be imprecise.

With regard to the creep model it has to be taken into account that for the elasto-plastic behaviour of the Opalinus clay the creep model uses an elasto-plastic model (Mohr-Coulomb) adapted for a homogeneous isotropic material. This approach may be less suitable to represent the mechanical matrix and bedding behaviour of the strongly anisotropic Opalinus clay and it rather overestimates the strength of the Opalinus clay.

As Figure 3-18 shows, after 730 days - including one year of simultaneous heating at both heaters -, the stresses in the host rock surrounding heater 2 approach failure, and the EDZ in the drift affects more zones. The EDZ has a greater extent close to the boreholes.

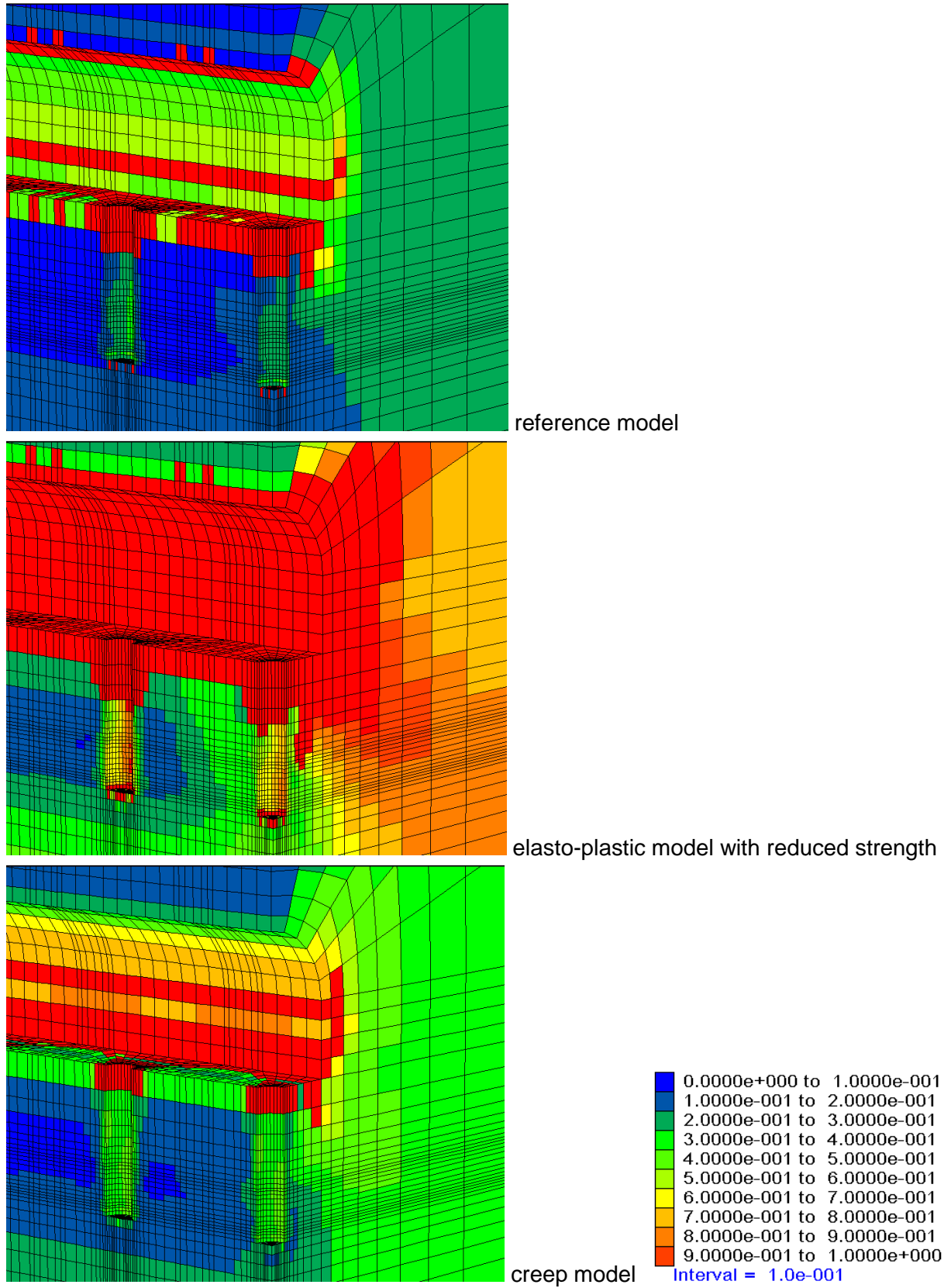
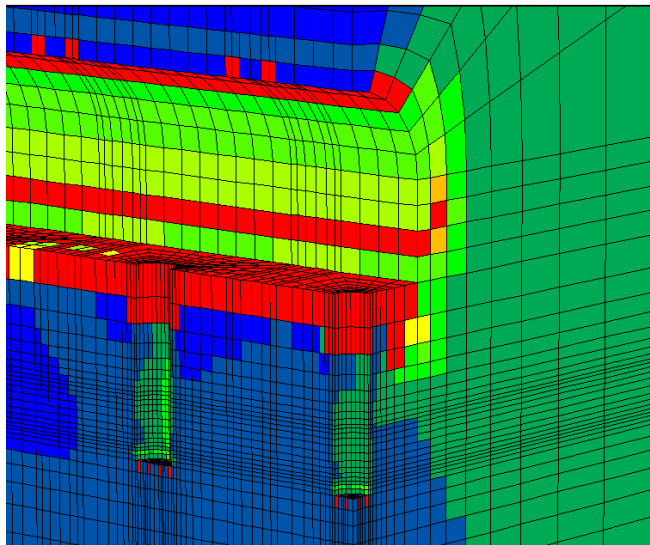
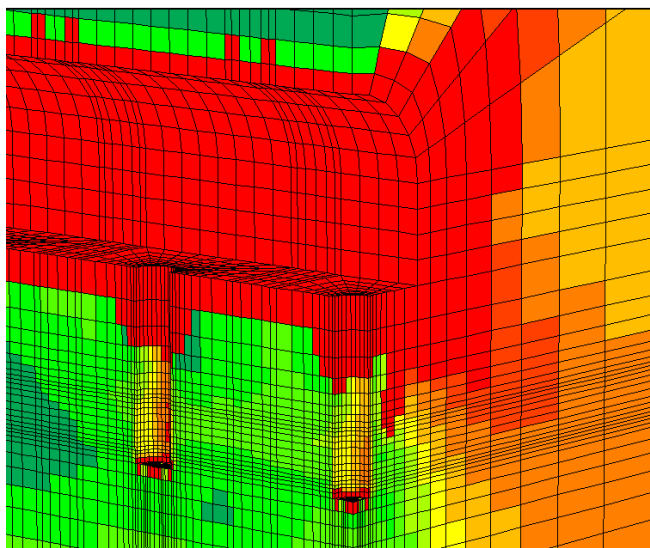


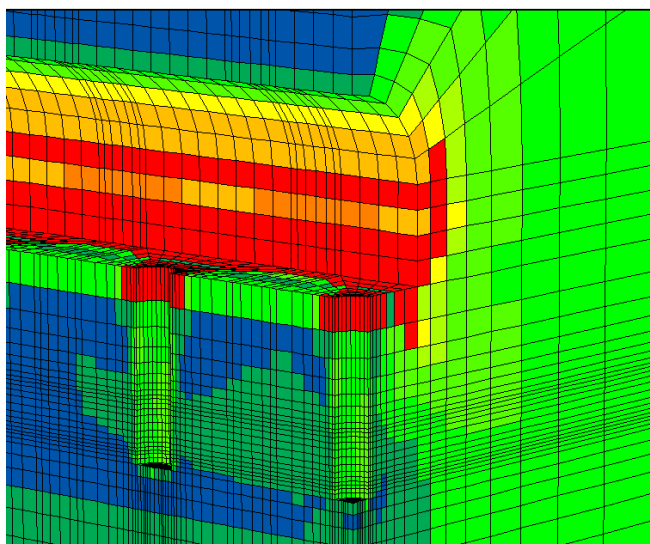
Figure 3-17: Stress/strength ratio [-], t = 365 d, heaters and buffer are not displayed



reference model



elasto-plastic model with reduced strength



creep model

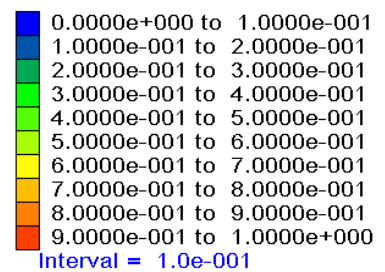


Figure 3-18: Stress/strength ratio [-], t = 730d, heaters and buffer are not displayed

A further point of interest was the question if borehole 2 needed to be stabilised during the one-year period it was left open. Figure 3-19 shows the stress/strength ratio for borehole 2 at

t = 365 d. The simulation results show that in all three mechanical model layouts there is a destabilisation around the top of the borehole which is largest in the elasto-plastic model with reduced strength (~2 m) and smallest in the creep model (~1 m). The reference model exhibits an EDZ of ~1.3 m depth close to the borehole. Additionally, at reduced strength properties a failure occurs in borehole 2 at the elevation where heater 2 is to be positioned (z = -3.65 m, mid of cask), (compare Figure 3-19).

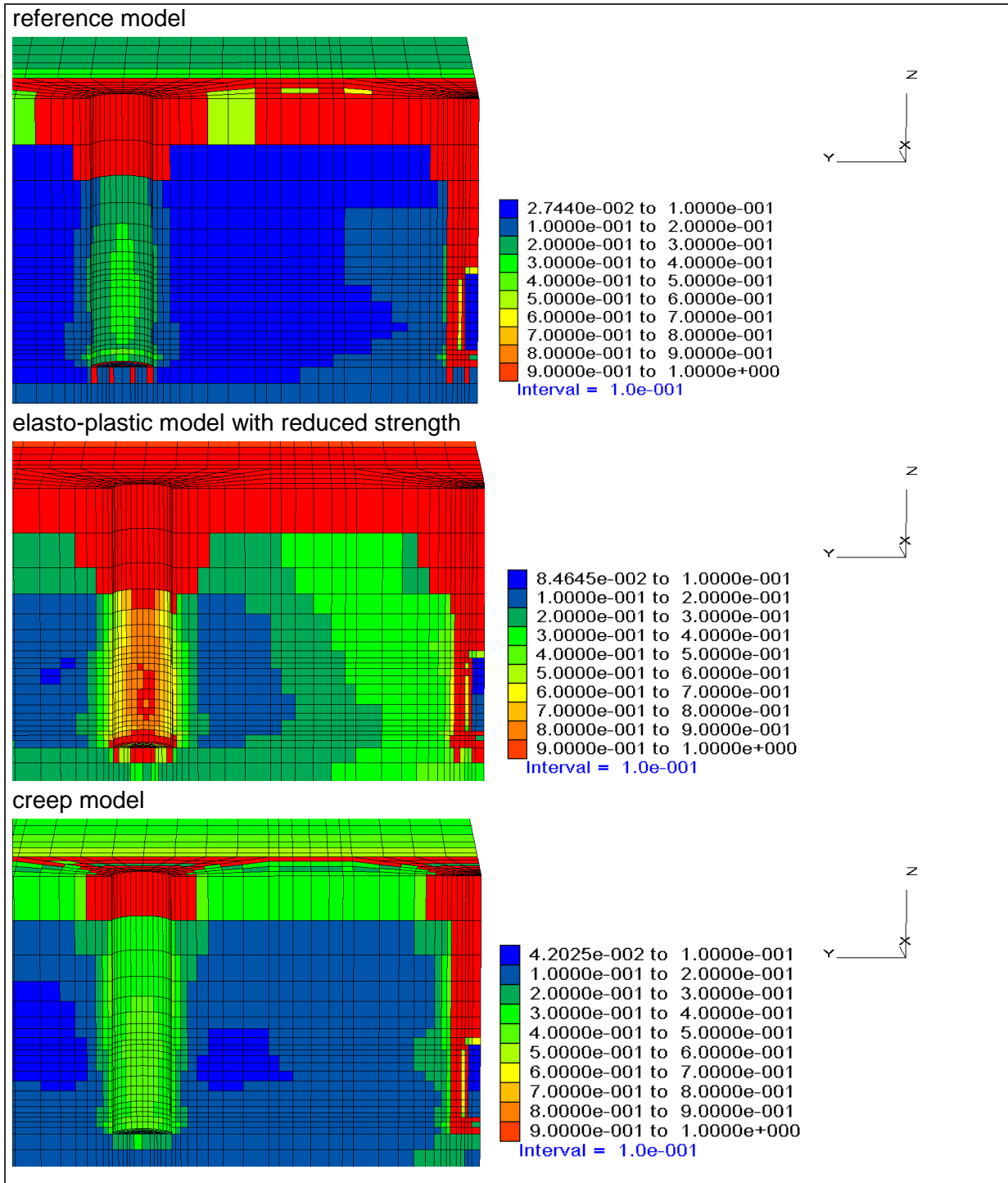


Figure 3-19: Stress/strength ratio [-] at borehole 2, t = 365d

Figure 3-20 shows the stress/strength ratio in a horizontal plane at a depth of 3.65 m. The load acting on the borehole contour is anisotropic with higher values perpendicular to the drift axis. The failure state is reached only in the elasto-plastic model with reduced strength properties. The failure zone comprises the model zones adjacent to the borehole contour. These zones have a horizontal extent of ~10 cm, which is the maximum extent of the failure zone.

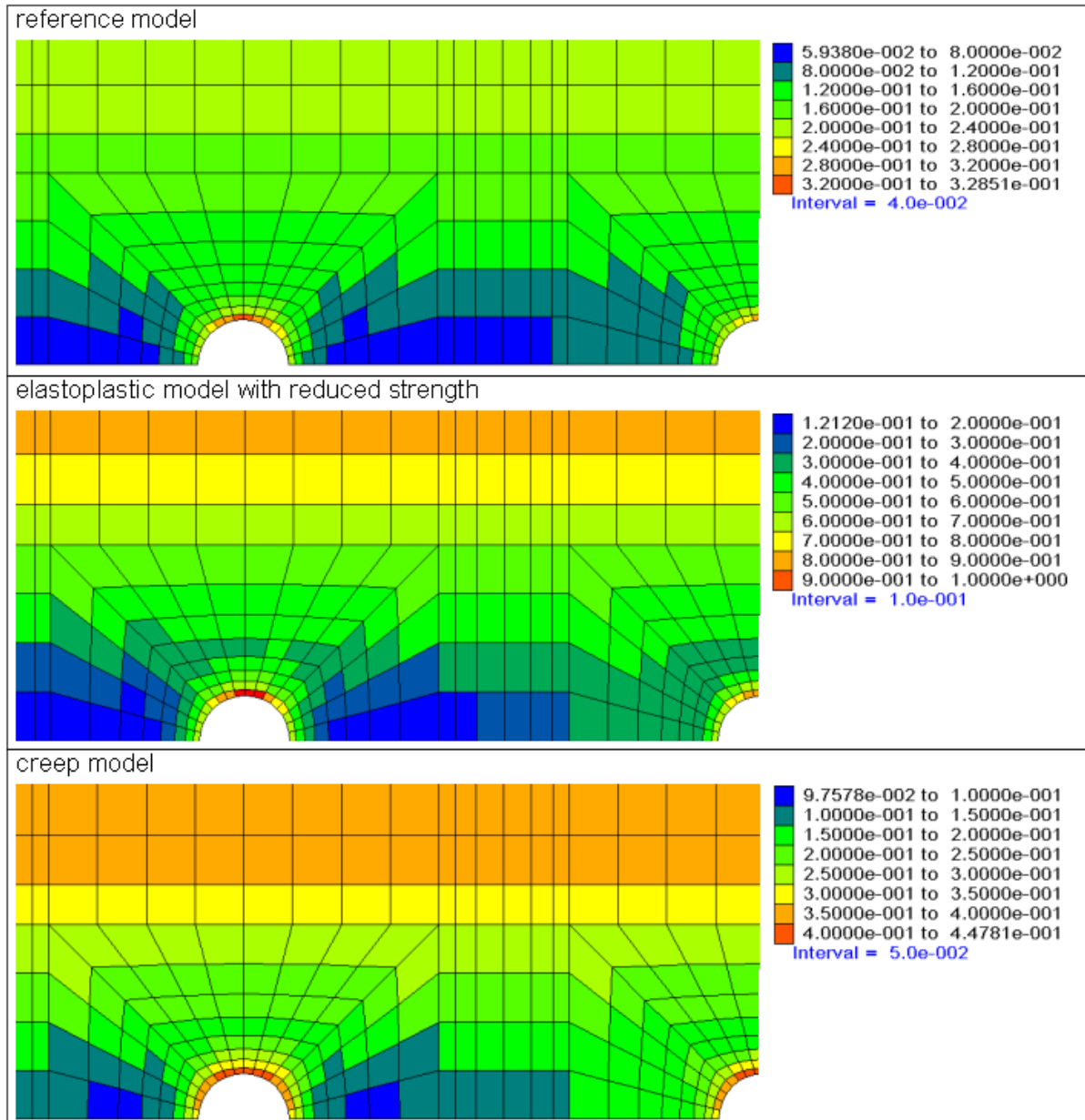
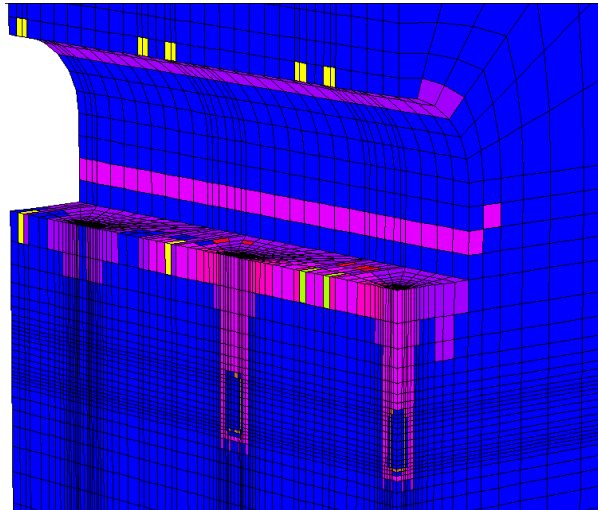


Figure 3-20: Stress/strength ratio [-] around the boreholes in a horizontal plane, $z = -3.65$ m, $t = 365$ d

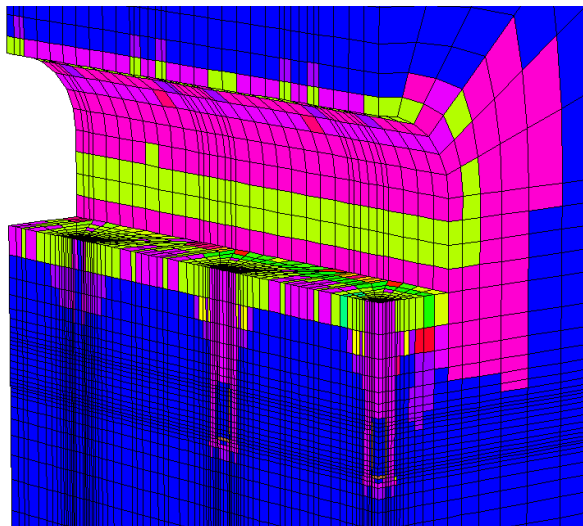
Figure 3-21 shows the failure mode at the end of the test (730 d); the different colours mark different failure modes, “u” indicates bedding failure and “n” denotes the present state whereas “p” stands for the past state. In the drift walls shear failure dominates while in the drift floor and roof mainly tensile forces cause failure.

reference model



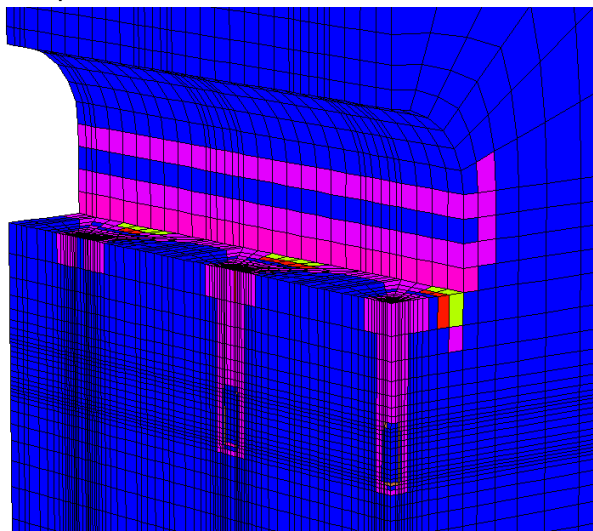
- None
- shear-n shear-p
- shear-p
- tension-n tension-p
- tension-n tension-p u:shear-p
- tension-p
- tension-p u:shear-p
- tension-p u:shear-p u:tension-p
- u:shear-n u:shear-p
- u:shear-p
- u:shear-p u:tension-p

elasto-plastic model with reduced strength



- None
- shear-n shear-p
- shear-p
- shear-p tension-p
- shear-p tension-p u:shear-n u:shear-p
- shear-p tension-p u:shear-n u:shear-p u:tension-p
- shear-p tension-p u:shear-p
- shear-p tension-p u:shear-p u:tension-p
- shear-p u:shear-n u:shear-p
- shear-p u:shear-n u:shear-p u:tension-p
- shear-p u:shear-p
- shear-p u:shear-p u:tension-p
- tension-n tension-p
- tension-n tension-p u:shear-p u:tension-p
- tension-p
- tension-p u:shear-n u:shear-p u:tension-p

creep model



- None
- shear-n shear-p
- shear-p
- shear-p tension-p
- tension-n tension-p
- tension-p

Figure 3-21: Plasticity indicators, t = 730 d

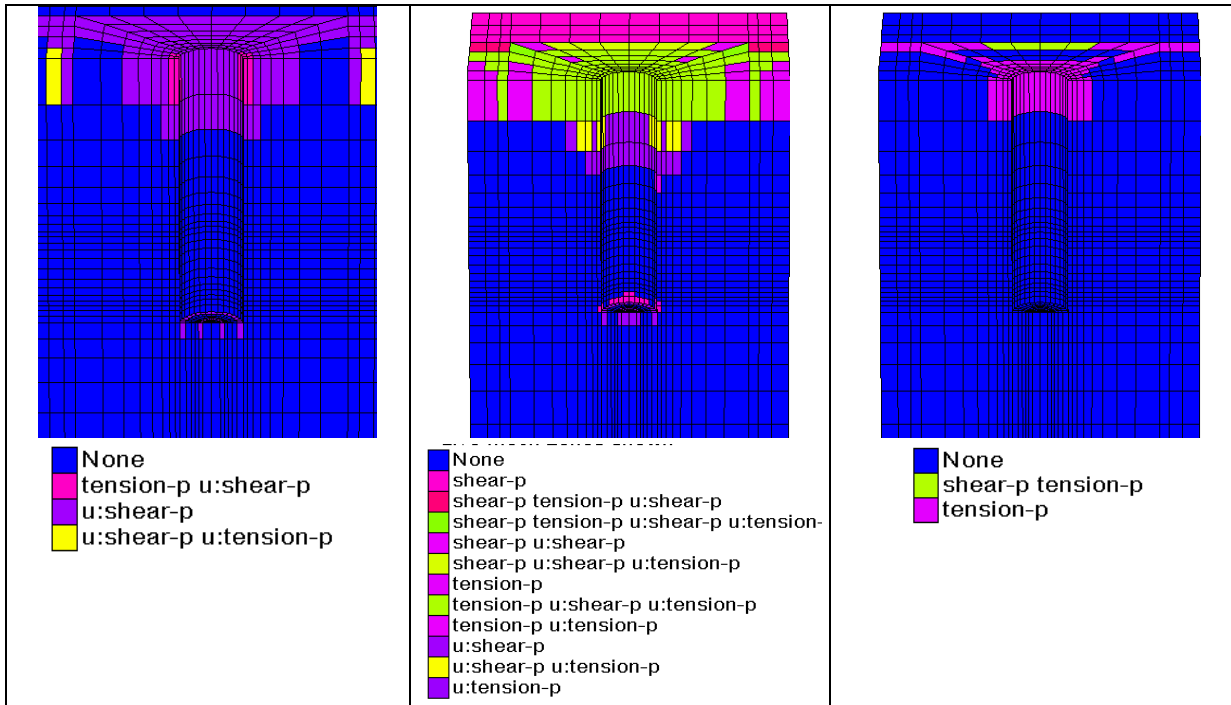


Figure 3-22: EDZ surrounding borehole 2 after borehole drilling $t = -30 d$ (left: reference model, centre: elasto-plastic model with reduced strength, right: creep model)

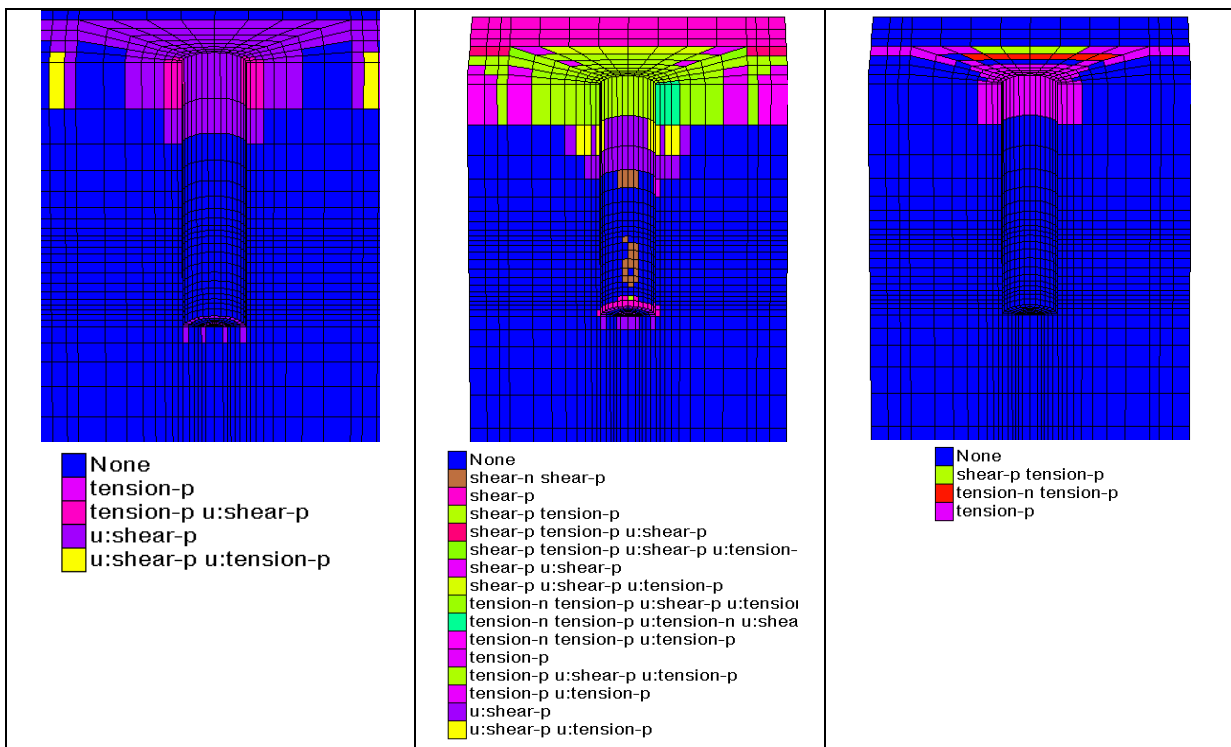


Figure 3-23: EDZ surrounding borehole 2 at $t = 365 d$ (left: reference model, centre: elasto-plastic model with reduced strength, right: creep model)

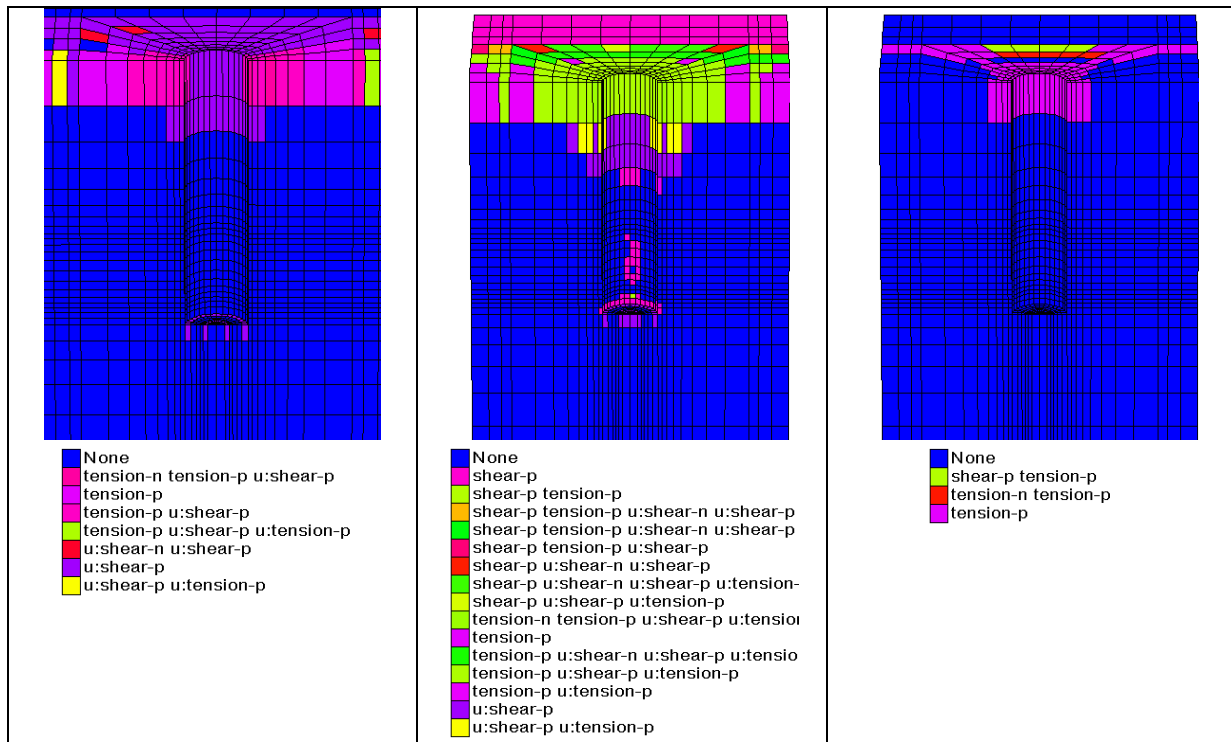


Figure 3-24: EDZ surrounding borehole 2 at $t = 730$ d (left: reference model, centre: elasto-plastic model with reduced strength, right: creep model)

3.2.2.3 Displacements

3.2.2.3.1 Displacements in the Niche

As a consequence of stress release after excavation, uplift of the drift floor occurs. The resulting displacements in the open borehole 2 up to $t = 365$ d is caused by stress release and thermal expansion induced by heating in borehole 1 (compare, i.e. Figure 3-25 and the polar diagrams in, i.e. Figure 3-29 and Figure 3-30). Both processes cause uplift of the drift. The latter also causes displacements towards the open borehole 2. The largest displacement resulted from the elasto-plastic model with reduced strength properties, the smallest displacements were exhibited by the reference model (Figure 3-25, Figure 3-26, Table 3-6).

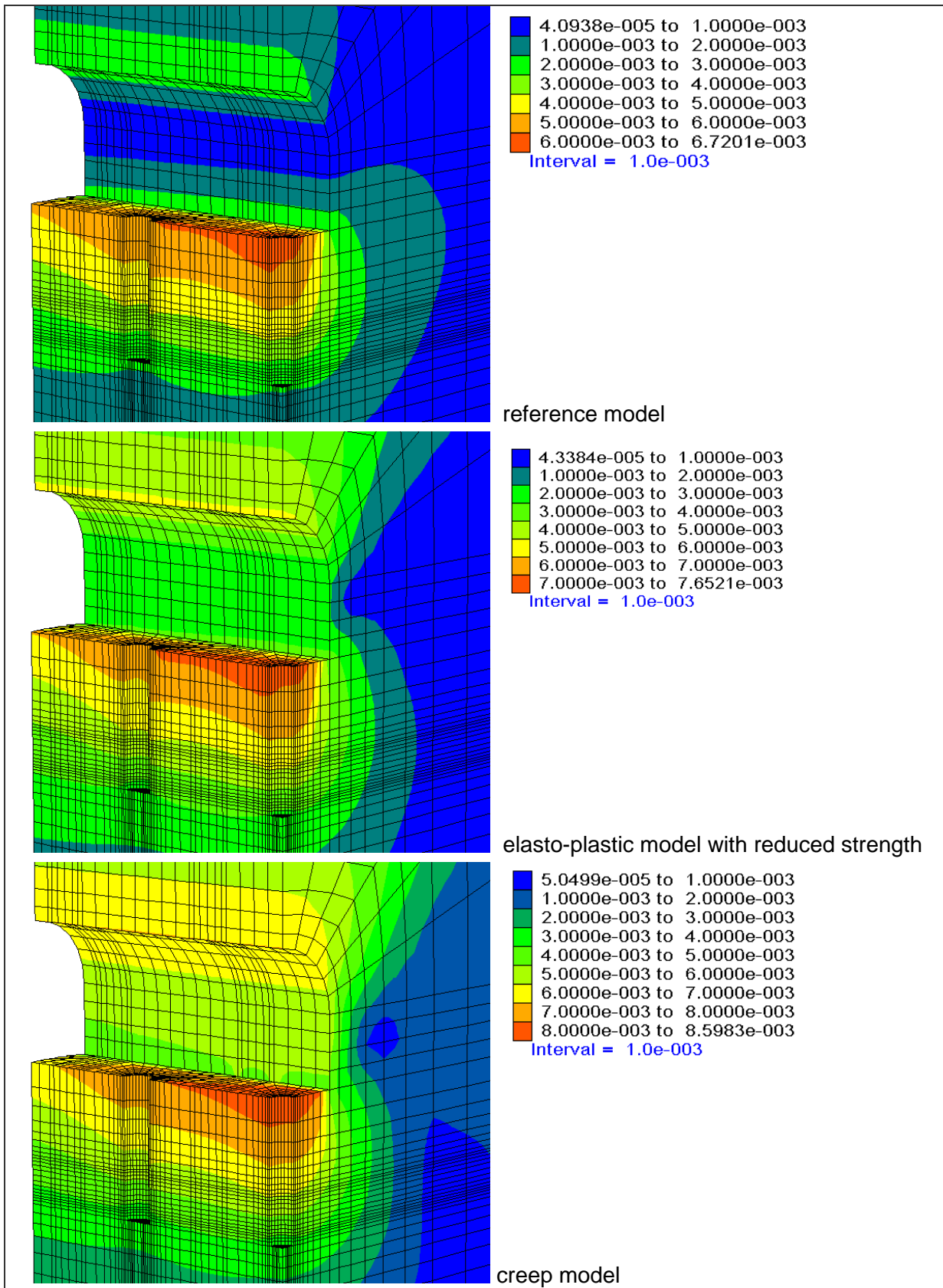


Figure 3-25: Displacements in the drift [mm], $t = 730$ d

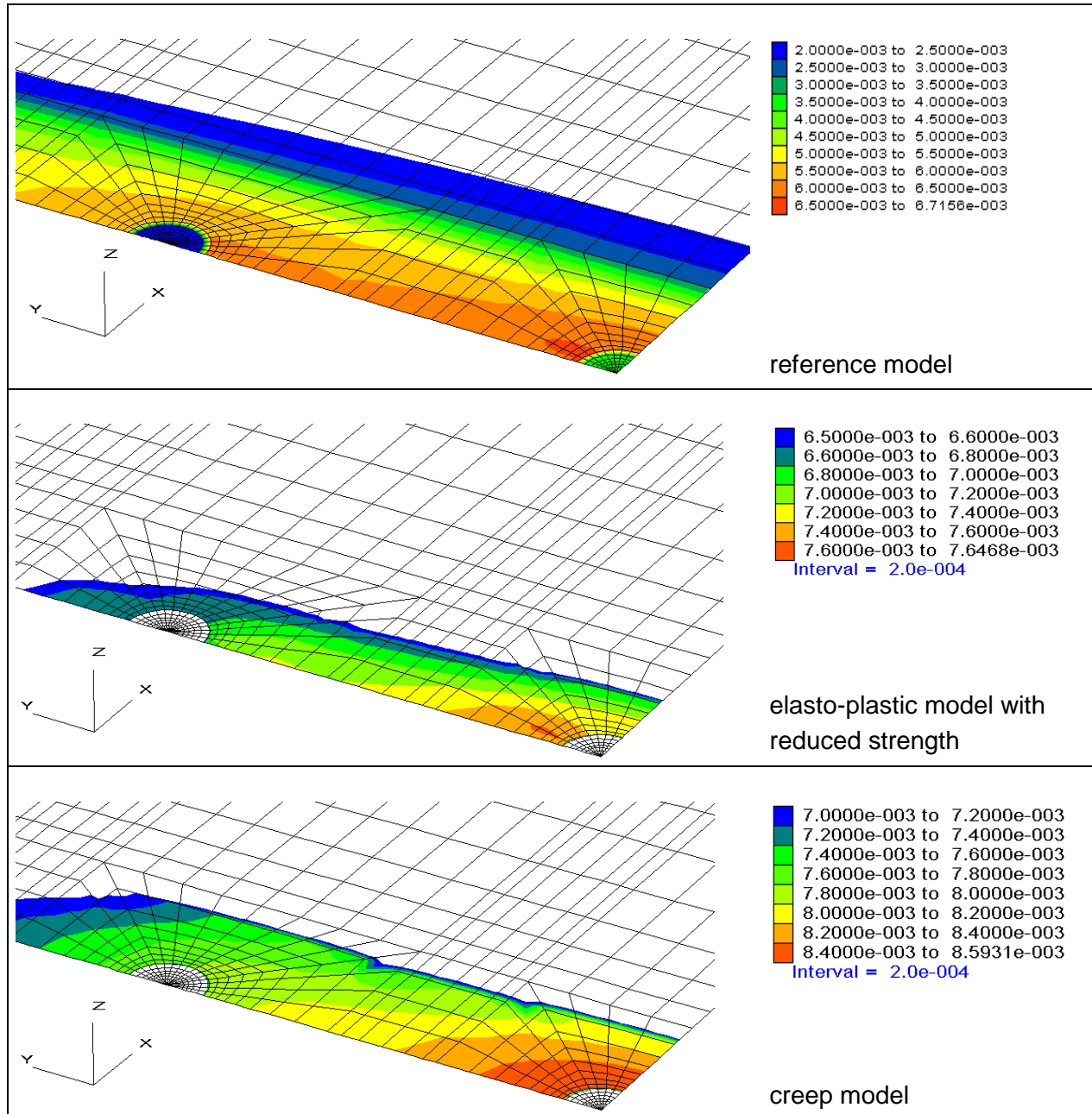


Figure 3-26: Displacement [m] in the drift floor

Table 3-6: Minimum and maximum displacements [mm] of the nodes within the zones adjacent to the drift

	reference model [mm]	elasto-plastic model with reduced strength [mm]	creep model [mm]
Roof	1.5 – 2.7	3.5 – 5.1	6.4 – 7.0
Wall	0.4 – 3.0	2.1 – 3.7	3.9 – 6.4
Floor	2.1 – 6.7	2.2 – 7.7	2.4 – 8.6

Roof (z: 3.517 – 4.7, x: 0 – 2.255), Wall (z: 0 – 3.517, x: 0 – 2.72), Floor (z: -0.7 – 0, x: 0 – 2.255)

3.2.2.3.2 Displacements in the Boreholes

The following polar diagrams show the top view of the boreholes for three different layouts (reference model, elasto-plastic model with reduced strength and creep model). In the polar diagrams, the borehole diameters at two horizons and at different time stages are plotted:

horizons:

- $z = 0$ m (drift floor),
- $z = -3.65$ m (midpoint heater)

time stages:

- prior to the drift excavation (- 486 d),
- after borehole drilling (-30 d),
- after borehole drilling and 30 days of drainage (0 d),
- after 183 days of heating at Borehole 1 (183 d), after 365 days of heating at Borehole 1 (365 d),
- after one further year with simultaneous heating at both heaters (730 d)

The maximum borehole displacement has a magnitude of ~1.5 mm. In all mechanical model layouts the development of the borehole contours is similar:

Borehole 1, cf. Figure 3-27, Figure 3-28, Figure 3-31, Figure 3-32, Figure 3-35, Figure 3-36

The dark blue graph represents the original borehole contour.

An instantaneous **elasto-plastic** response after borehole excavation can be observed ($t = -30$ d, light blue graph); in the two model layouts without consideration of creeping, the borehole is widened within the drift floor perpendicular to the drift axis, whereas in the deeper borehole section, close to the heater ($z = -3.65$ m), the borehole diameter shrinks. In the creep model the borehole shrinks at the level of the borehole mouth as well as in the deeper borehole section. The drainage of the boreholes does not significantly influence the displacements ($t = 0$ d, pink graph).

When **heating** at borehole 1 begins, the borehole contour is extended (yellow and red graph). The heating at borehole 2 results in a deformation of borehole 1 perpendicular to the drift axis (green graph).

Borehole 2, cf. Figure 3-29, Figure 3-30, Figure 3-33, Figure 3-34, Figure 3-37, Figure 3-38

The dark blue graph represents the original borehole contour.

Due to instantaneous **elasto-plastic** response after borehole drilling, the borehole diameter shrinks ($t = -30$ d, light blue graph). The reduction of the borehole diameter is more pronounced in its bottom segment (at $z = -3.65$ m). The drainage of the boreholes does not significantly influence the borehole displacements ($t = 0$ d, pink graph).

Due to **heating** at borehole 1, borehole 2 moves away from borehole 1 ($t = 183$ d, yellow graph and $t = 365$ d, red graph). Heating at borehole 2 causes an extension of the borehole diameter ($t = 730$ d, green graph).

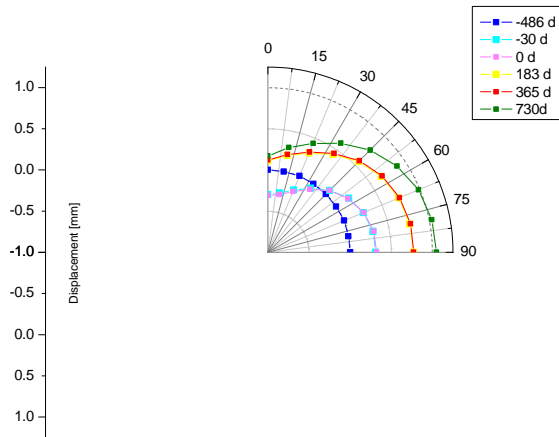


Figure 3-27: Reference model, borehole 1, z = 0 m

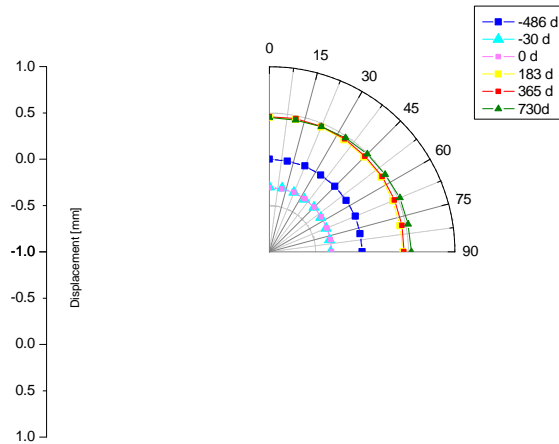


Figure 3-28: Reference model, borehole 1, z = -3.65 m

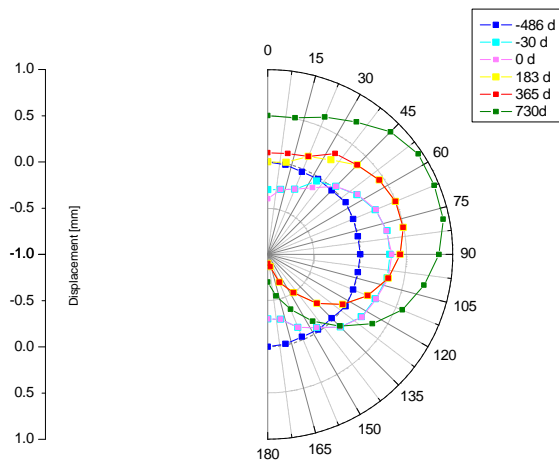


Figure 3-29: Reference model, borehole 2, z = 0 m

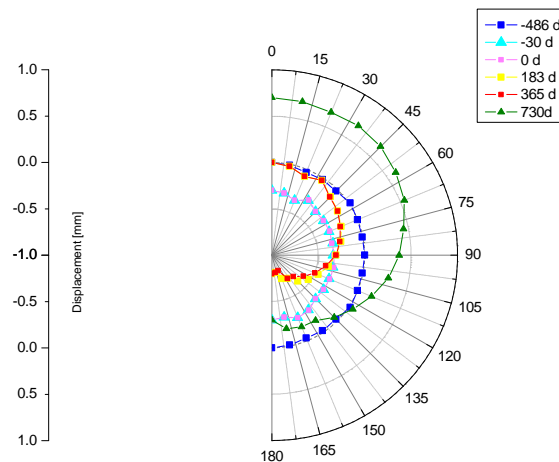


Figure 3-30: Reference model, borehole 2, z = -3.65 m

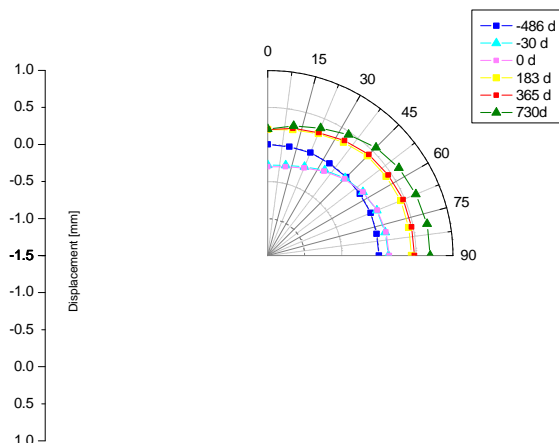


Figure 3-31: Model with reduced strength properties, borehole 1, z = 0 m

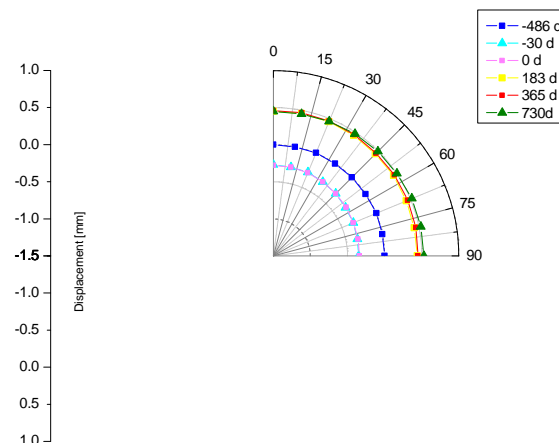


Figure 3-32: Model with reduced strength properties, borehole 1, z = -3.65 m

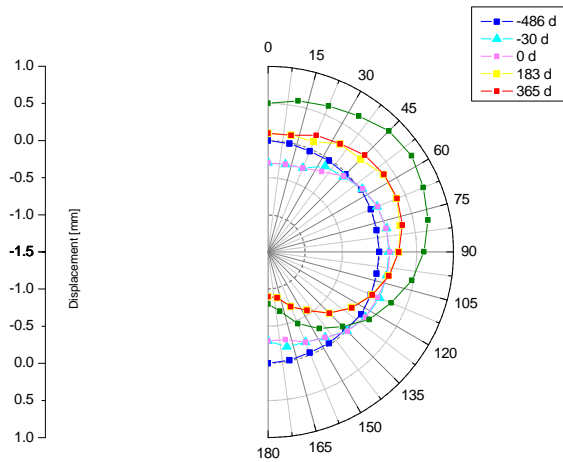


Figure 3-33: Model with reduced strength properties, borehole 2, z = 0 m

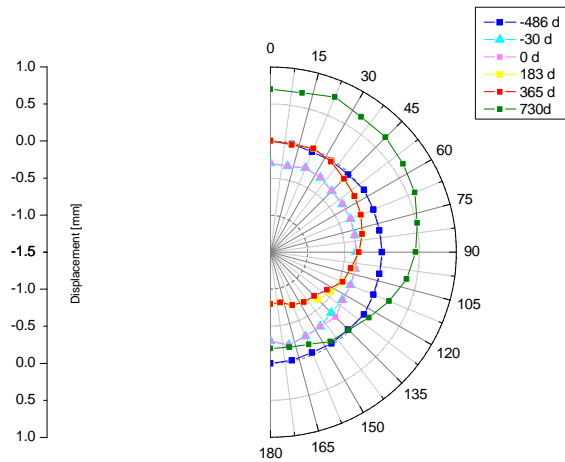


Figure 3-34: Model with reduced strength properties, borehole 2, z = -3.65 m

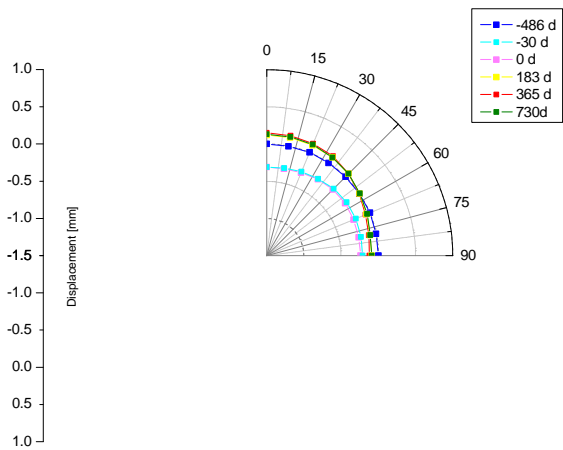


Figure 3-35: Creep model, borehole 1, z = 0 m

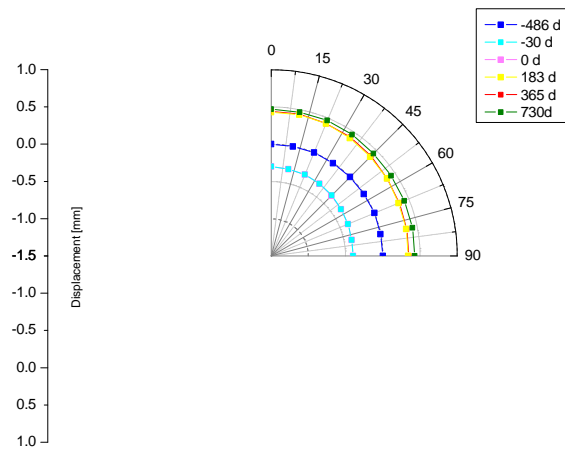


Figure 3-36: Creep model, borehole 1, z = -3.65 m

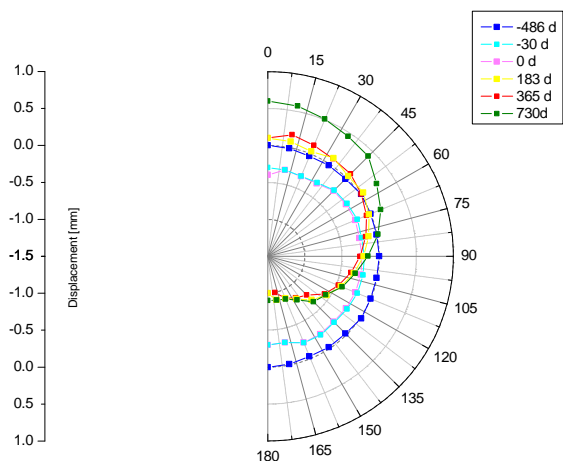


Figure 3-37: Creep model, borehole 2, z = 0 m

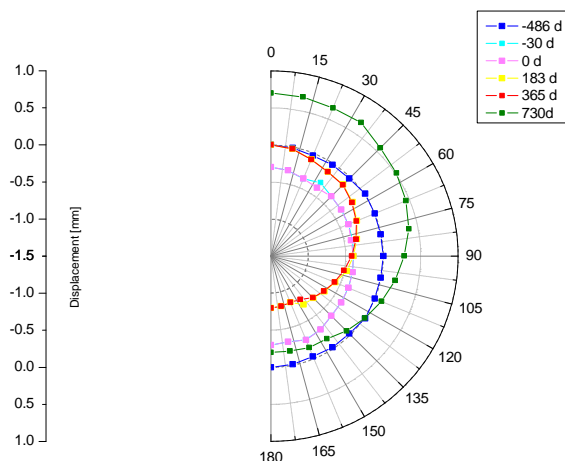


Figure 3-38: Creep model, borehole 2, z = -3.65 m

3.2.2.4 Pressure

In order to evaluate the load on the heater surface, the radial total pressure equal to normal stress is recorded at monitoring zones within the heaters at three different levels (compare Figure 3-39). The pressure recording was carried out for the reference model layout (compare section 3.1.6).

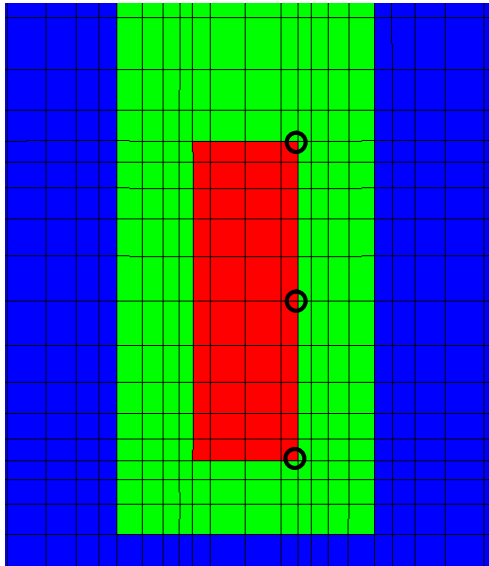


Figure 3-39: Pressure monitoring levels at borehole 2. The same monitoring levels apply to borehole 1.

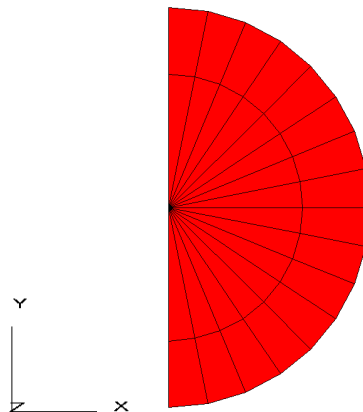


Figure 3-40: Pressure monitoring zones at one monitoring level at heater 2.

Figure 3-41 - Figure 3-44 demonstrate the development of radial stress acting on the heater surface for highly compacted bentonite during the course of the test. For $t < 0$, the graphs show the stresses within the host rock prior to borehole drilling and heating.

After the heaters have been turned on, the radial stress acting on the heater surface increases due to thermal expansion. The largest loads occur in the centre of the heater at heater 1 (elevation $z = -3,6$ m), and at the heater bottom of heater 2. The maximum pressure

is obtained at the end of the simulation. The maximum pressure occurred at heater 1 at an elevation of -3,6 m, and the maximum pressure at heater 2 at an elevation of $z = -3,6$ m. The maximum calculated values are:

- for highly compacted bentonite: $P_{max} \approx 7.7$ to 9.1 MPa
- for granular bentonite (slightly compacted in-situ): **$P_{max} \approx 1.6$ to 1.7 MPa**

For the time being, it is intended to use granular bentonite with slight in-situ compaction.

It has to be taken into account that the heater, the surrounding bentonite buffer and the host rock are considered to be a continuum in the model, while in reality there may be joints due to construction, so that tractional linkage has to develop prior to loading. Therefore, the model may overestimate the load on the heater surface. As a comparison, the pressure measured within the bentonite buffer in the Äspö Hard Rock Laboratory was of a similar magnitude (SKB 2008).

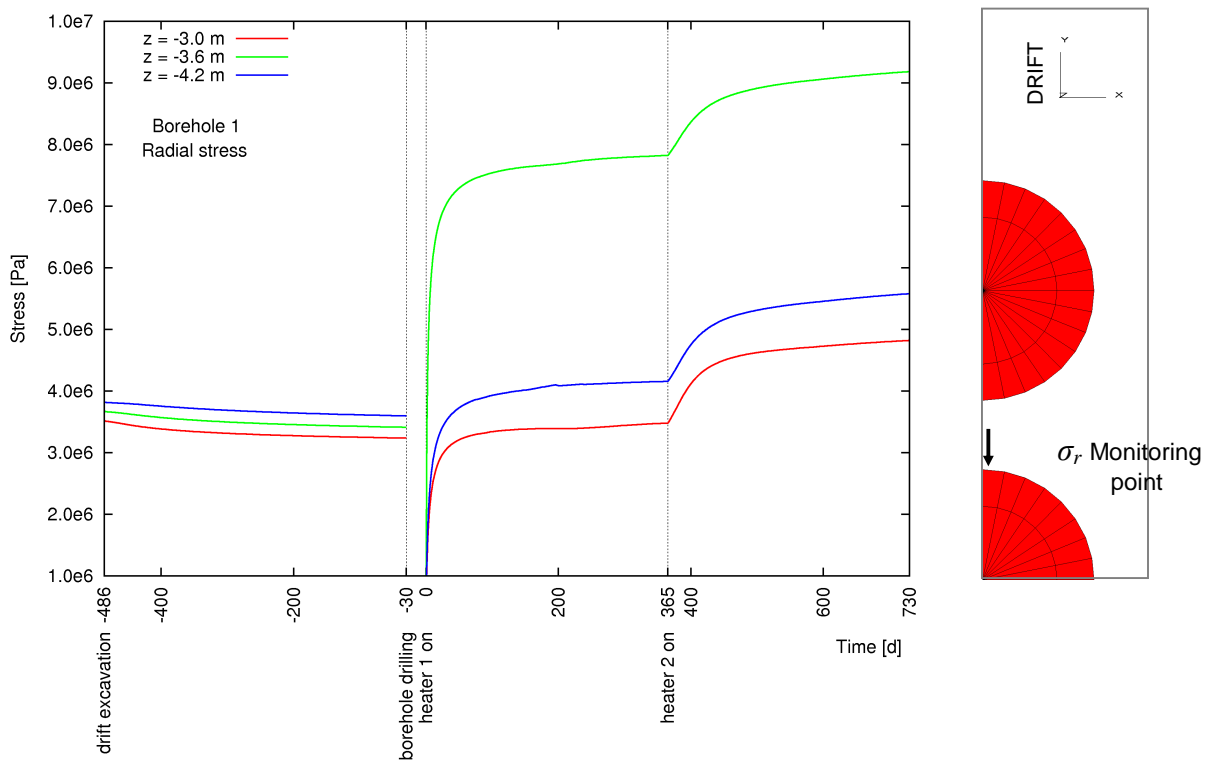


Figure 3-41: Heater 1: radial total pressure along the drift axis at different elevations (highly compacted bentonite)

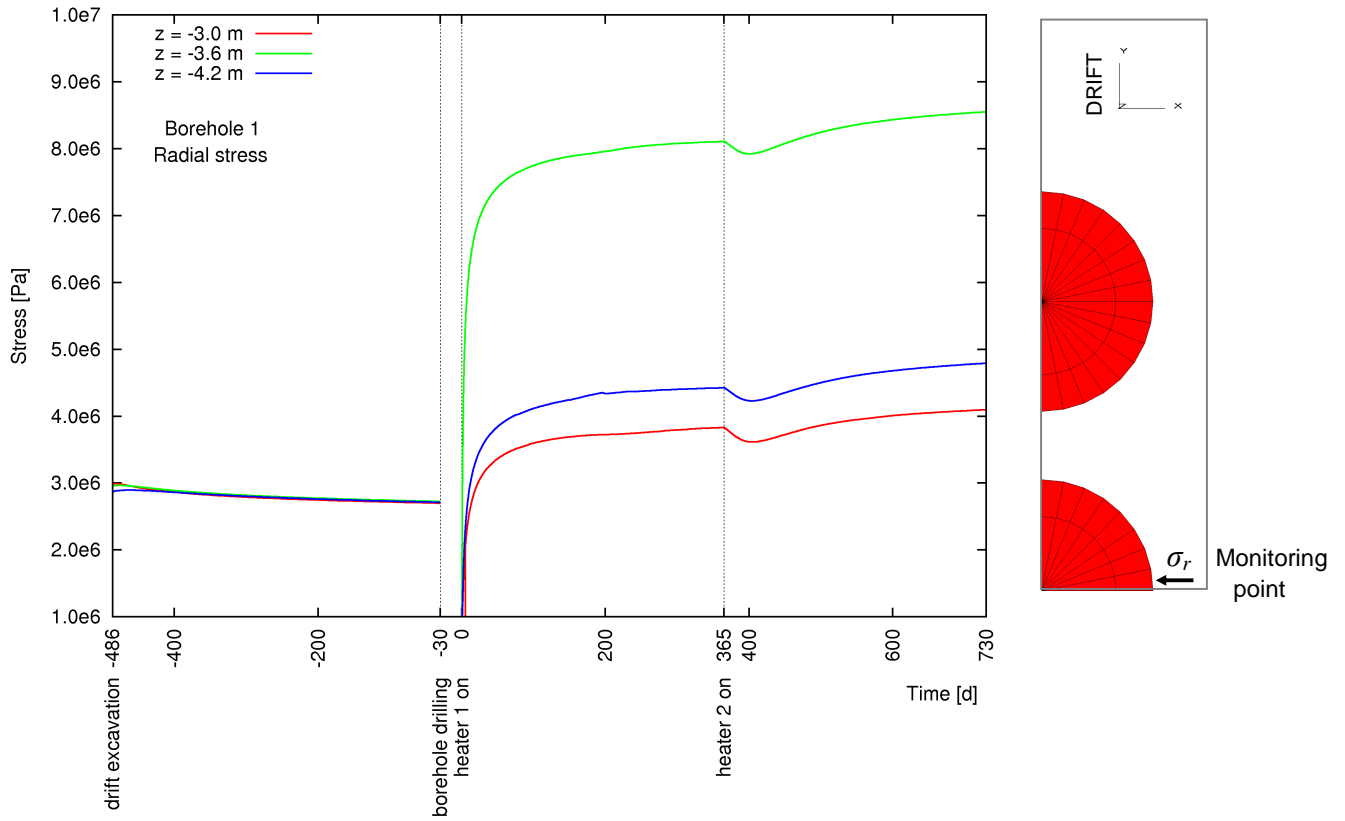


Figure 3-42: Heater 1: radial total pressure perpendicular to the drift axis at different elevations

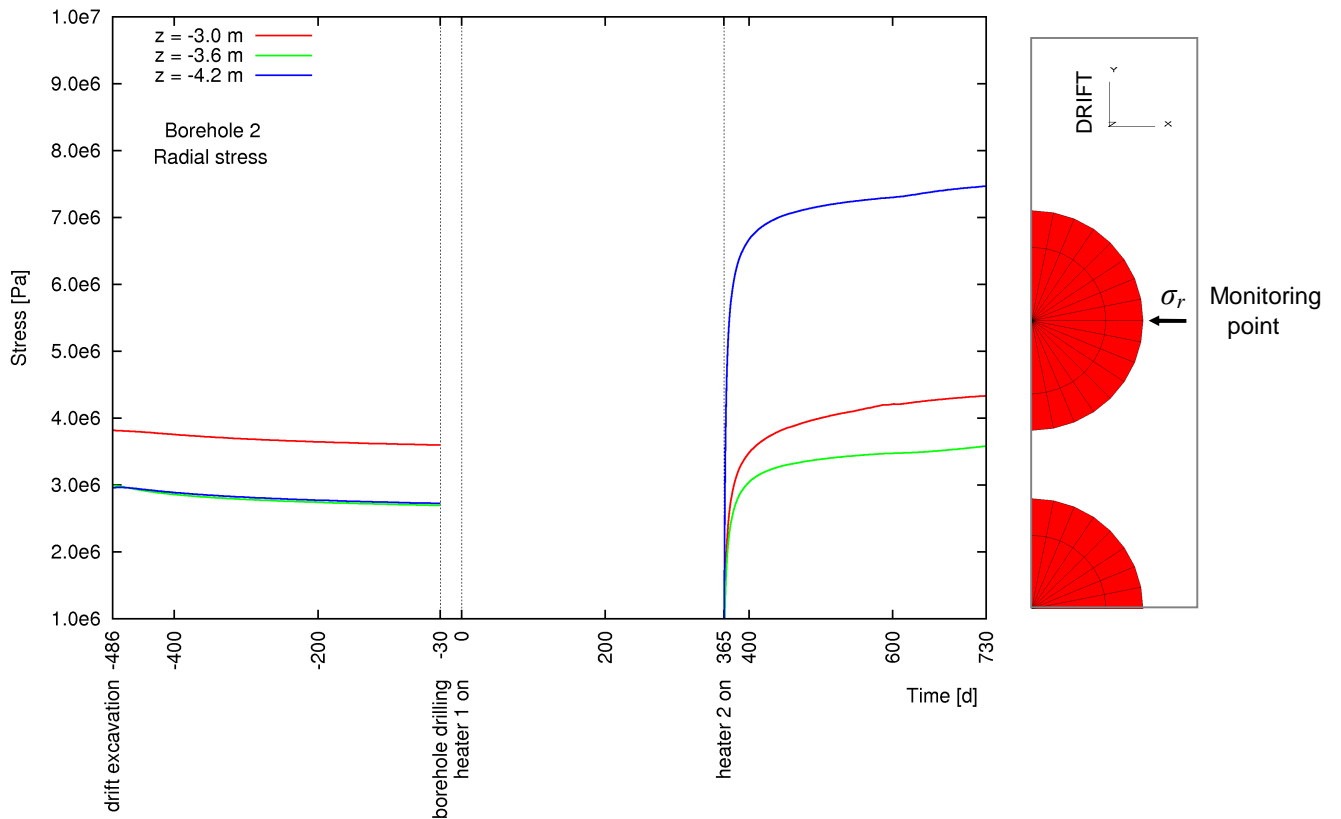


Figure 3-43: Heater 2: radial total pressure perpendicular to the drift axis at different elevations

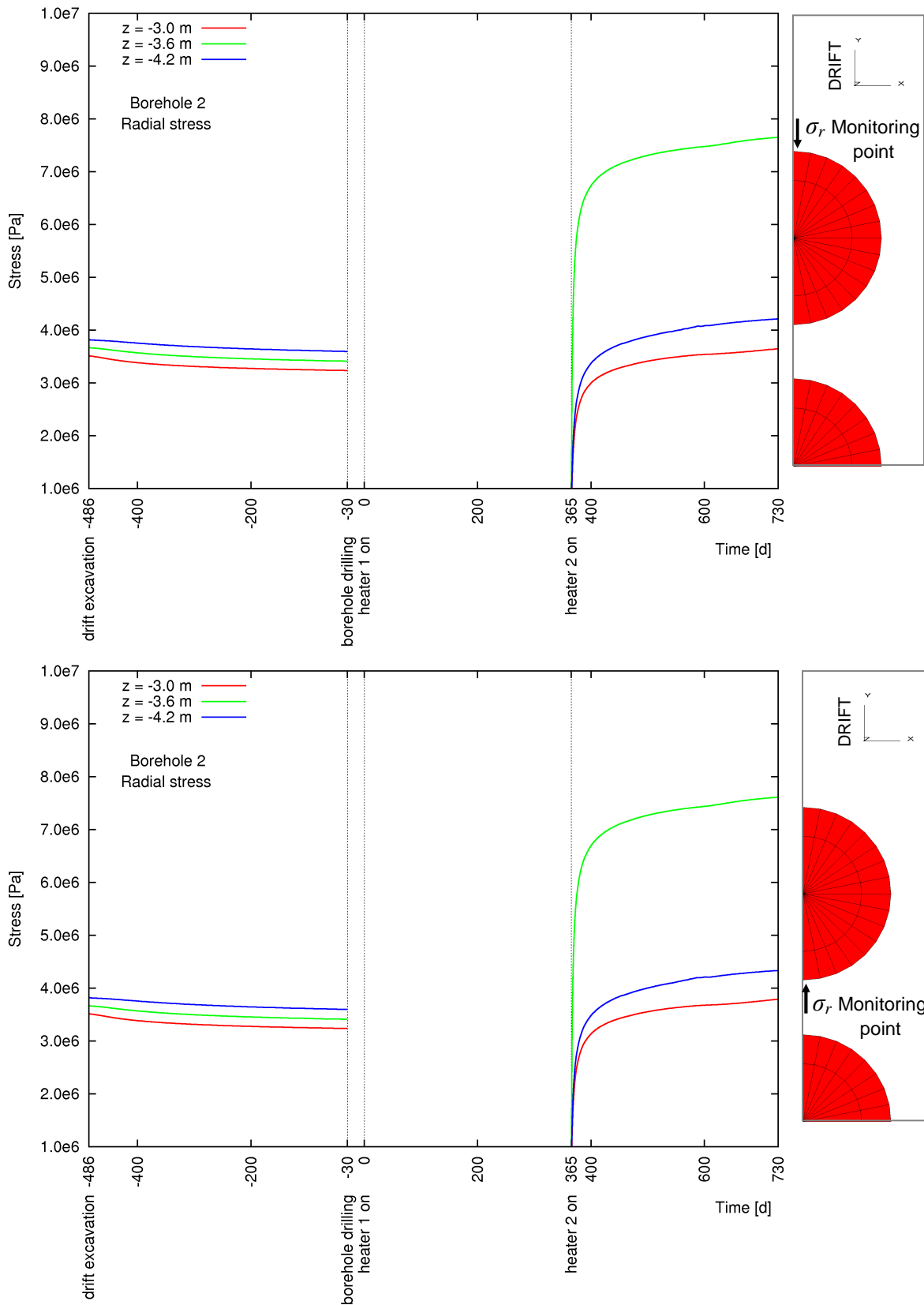


Figure 3-44: Heater 2: radial total pressure along the drift axis at different elevations

4 Measurement Concept and Experiment Schedule

The following gives a chronological overview of the preparatory and accompanying laboratory activities as well as of the individual phases of the experiment including the corresponding measurement campaigns.

4.1 Laboratory Investigation of Host Rock and Buffer Material

It is intended to carry out the TwisT experiment in the sandy facies of the claystone in the underground laboratory in Mont Terri where so far hardly any experiments have been carried out. For this reason, no measurement data regarding the thermal rock parameters of this material are available. Currently, it is assumed that the thermal conductivity is slightly higher than that of the more clayey facies. Selected rock samples are to be measured by means of a novel measuring equipment available at GRS as well as by means of a conventional, standard measuring equipment (Divided Bar). The latter is available at Geophysikalisch-Technisches Büro Clausthal, Prof. Buntebarth. After a comparison and plausibility validation of the measurement results of both measuring systems, the results are to be used as input parameters for a detailed projection of the experiment.

Investigation of the Opalinus clay (sandy facies)

Core samples of several boreholes will be taken from the rock at the location of the TwisT experiment in the URL Mont Terri and their thermal rock parameters will be determined in the laboratory. The thermal conductivity and diffusivity parallel and perpendicular to the bedding, the specific heat capacity as well as the thermal expansion are to be measured. The measurements parallel and perpendicular to the bedding will be used to determine the anisotropy factor. The thermal conductivity is of major importance for the development of the temperature field. This is why the thermal conductivity is determined as a function of fluid content and temperature, as both vary in the surrounding rock during the course of the experiment. As there are not sufficient data on the sandy facies, parameters concerning material strength (Young's modulus, Poisson's ratio, rupture strength) and hydraulic parameters (porosity, gas permeability), which are necessary for the THM modelling, will be determined as well.

Investigation of the bentonite-sand mixture (SB)

As previous laboratory investigations of the bentonite-sand material (SB) were always carried out at room temperature, additional measurements at temperatures relevant to a repository (and to the experiment) are required. This includes experiments regarding the temperature dependency of the hydraulic and mechanical behaviour of the SB material. For a more detailed assessment of the suitability of the selected material, an assessment of its capacity to dissipate heat in an adequate measure is required. The investigations will be carried out on a "naturally moist" clay-sand mixture with a clay content of 35% and a sand content of 65% as a function of the compaction degree. Comparative measurements will be carried out on material dried at a temperature of 105°C. As thermal parameters will be influenced by a temperature increase, the measurements will be carried out at varying ambient temperatures up to 80°C. The measurements will be carried out with measurement equipment available at GRS.

Investigations of the bentonite-graphite mixture (GB)

When the measurement results of the Opalinus clay of the sandy facies are available, bentonite-graphite mixtures with thermal conductivities of the same order of magnitude as those of the Opalinus clay are to be prepared. Test measurements are to determine the optimal mixing ratio for the experiment.

4.2 Preparation of the Experiment and Set-up

In preparation of the experiment, both, the two large-scale boreholes for the electric heaters as well as the monitoring boreholes will be drilled. A geological survey of the boreholes will be performed and they will be equipped with measuring systems to monitor the rock behaviour. Further sensors will be installed in the experiment niche for deformation measurements.

During a set-up phase, the rock behaviour without artificial heating will be recorded so that later, thermally-induced processes can be distinguished from purely hydromechanical effects. Microseismic measurements, especially to document the excavation damaged zone, complete the measuring concept.

4.2.1 Drilling of the Heater Boreholes

First, the two large-scale heater boreholes will have to be drilled. It is intended to assign this task to drilling companies that are highly experienced in drilling boreholes in claystone, e.g. the companies COFOR-COREIS and Schuetzeichel KG. The two large-scale boreholes are to be drilled in direct succession. The planning and organisation will be carried out by Geotechnical Institute Mont Terri (on-site management) on behalf of the project partners.

4.2.2 Geological Logging of the Heater Boreholes

After the boreholes have been drilled, a geological survey will be performed, again by Geotechnical Institute Mont Terri. The logging is to identify any weak zones (cracked zones), to detect strata with different lithologies, and to determine the exact orientation of the bedding. These data are important boundary conditions for both, the analysis of the experiment and the model generation.

4.2.3 Drilling and Equipping the Monitoring Boreholes

In the vicinity of the heater boreholes H1 and H2, monitoring boreholes will be drilled and equipped with sensors to measure mechanical rock displacements, temperatures, pore water pressures, and permeabilities. All boreholes foreseen for temperature and pore pressure measurements will be very small (2-3 mm) in order to minimize the rock disturbance. The boreholes will be arranged in a grid pattern which offers the following measurement means:

- monitoring the development of the pore water pressure especially between the two heater boreholes at three different depths (Figure 4-1)

- monitoring the temperature development at approx. 350 points in a rock zone shaped like a rectangular cuboid around the heaters (Figure 4-2)
- monitoring the rock deformation parallel to the heater boreholes as well as in radial direction (Figure 4-2, Figure 4-3). In order to achieve the latter, it is intended to drill two boreholes from the adjacent gallery 08 (Figure 2-1), which will be slightly inclined towards the heaters and furnished with high-resolution extensometers.

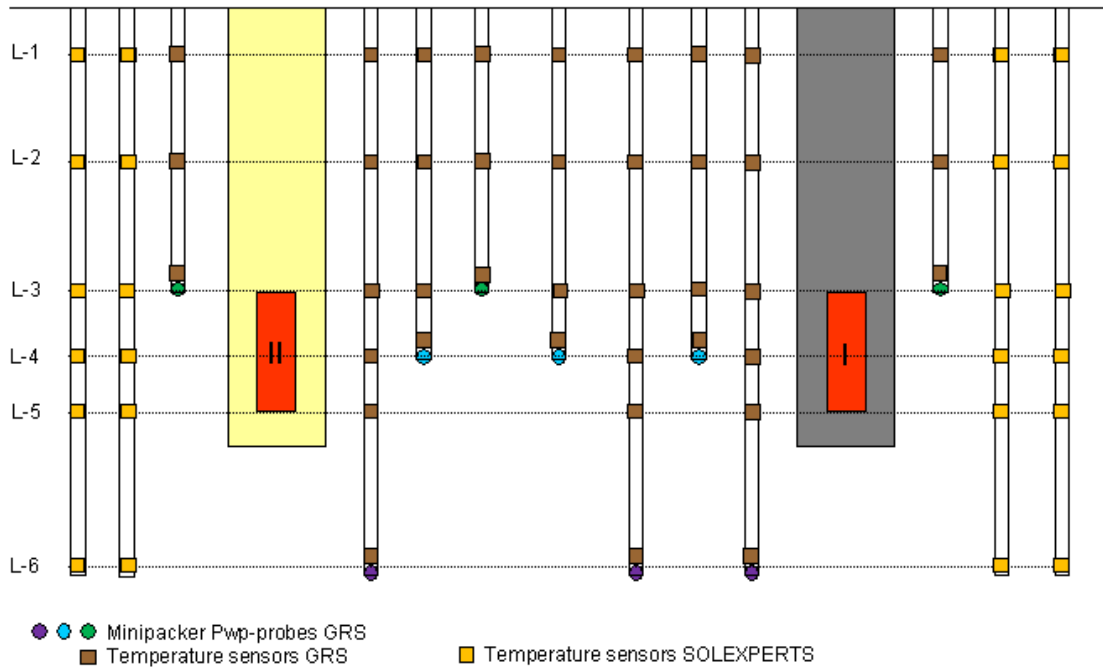


Figure 4-1: Borehole profile for monitoring pore water pressure (not to scale)

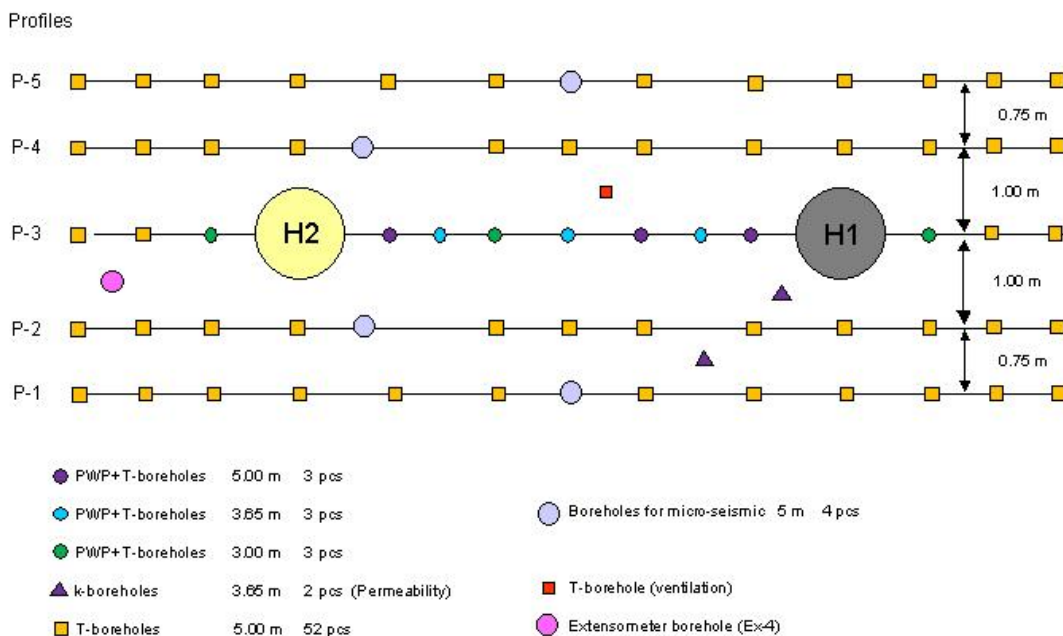


Figure 4-2: Location of the monitoring boreholes - top view - (not to scale)

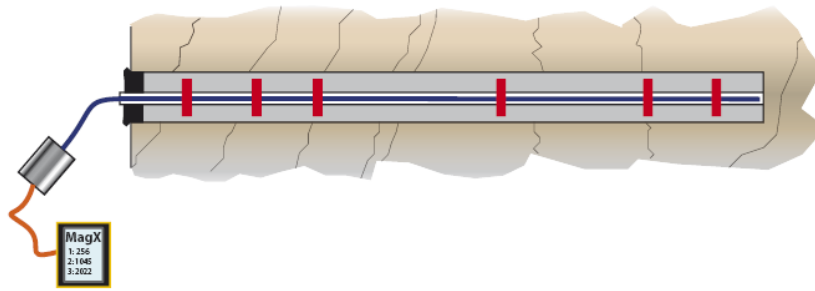


Figure 4-3: Extensometer for deformation measurements

Supplementary to the deformation measurements it is intended to have the company Swisstopo perform uplift measurements of the floor of the niche in order to determine the uplift caused by thermal expansion. As the heating will continue for two years, there will be an overall deformation and thermally-induced convergence of the niche. This convergence is to be measured as well.

4.2.4 Fabrication and Testing of the Heaters

The two heaters for the experiment will be designed, fabricated, and tested by the company Aitemin in Spain. The company is highly experienced in this field as it has already equipped and performed several in-situ experiments with heaters, some of them still ongoing.

The monitoring and control units of the heaters are designed in a redundant configuration in order to keep total system failures at a minimum. The outside of the heaters will be furnished with temperature and pressure sensors. The temperature sensors are to monitor the temperature at the surface of the heaters, which is in direct contact with the bentonite, and is not to exceed the thermal boundary conditions of 100°C. The heaters can be temperature-controlled or power-controlled. The mode of operation can be changed at any time during the experiment, if required. The outside of the heaters will also be furnished with pressure sensors in order to monitor the thermo-mechanical load on the dummy containers, i.e. the heaters.



Figure 4-4: Installation of a heater at the Äspö URL (Aitemin)

The heaters can either be controlled directly on site or remotely via the internet by authorized users. The measurement values of all connected sensors can also be viewed on the internet. Figure 4-4 shows a heater at the Äspö URL being installed by Aitemin. The installation at the URL Mont Terri will be similar.

4.2.5 Geotechnical Measurements in the Set-up Phase

In order to be able to identify the part of the thermo-hydro-mechanical behaviour of the Opalinus clay that is due to the artificial heating, it is necessary to determine and record the initial state of the system before heating. It is known that the rock mass in the URL is not a static system but is subject to continual changes to a greater or lesser extent, especially in terms of rock deformation. For this reason, it is intended to not only record the initial state of the system, similar to taking a snapshot, but to particularly record long-term trends in the THM behaviour. In addition to stress redistributions, cyclic variations of the ventilation may also lead to recurring changes in the vicinity of the cavities. Recording these processes is indispensable for the determination of correct initial and boundary conditions for the modelling.

4.2.6 In-situ Measurement of the Thermal Conductivity

In addition to the planned laboratory measurements to determine the thermophysical rock parameters of the sandy facies of the Opalinus clay, in-situ measurements by means of suitable equipment are to be carried out as well in order to determine the thermal conductivity, the parameter fundamental to the temperature distribution. These measurements are to be taken along several horizontal and vertical profiles Figure 4-5 by Geophysikalisch-Technisches Büro Clausthal, Prof. Buntebarth in order to identify anisotropic effects as well as any local heterogeneities. A comparative analysis of these measurements against the laboratory measurements of core material is to be performed.

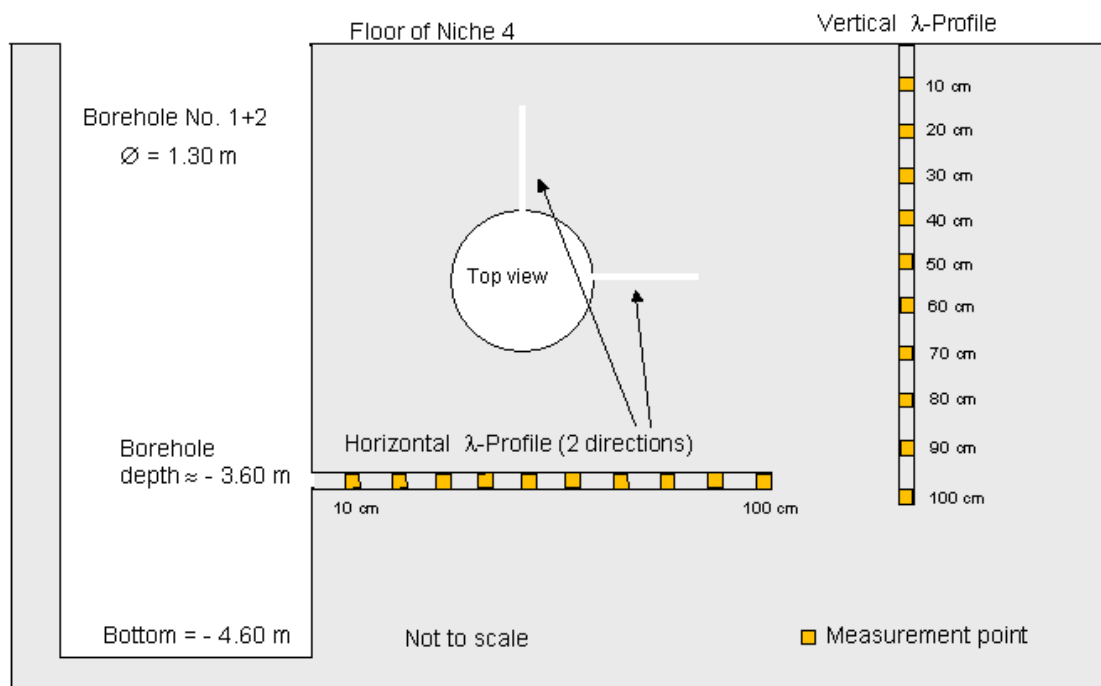
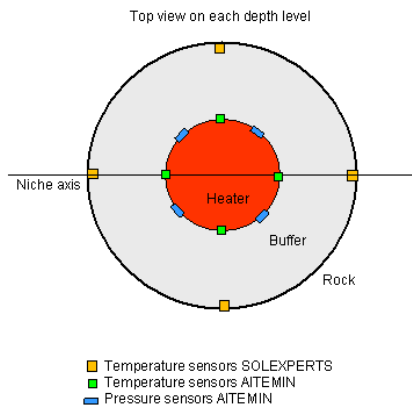


Figure 4-5: Measurement profiles for thermal conductivity (λ) determination

4.2.7 Installation of Heater 1 and of the GB Buffer Material

After the preliminary measurement phase has been completed, the first borehole will be equipped with the first heater which is subsequently connected and subjected to a function test.



The borehole wall will be equipped with temperature sensors along 4 vertical profiles. A top view of the borehole is shown in Figure 4-6. The void space around the heater will be filled with bentonite-graphite granules which will be slightly compacted. Subsequently, the void above the heater up to the floor of the niche will also be back-filled with bentonite-graphite granules which will be compacted slightly and in layers. The borehole will then be sealed by means of a steel plate which will be fastened to the floor of the niche.

Figure 4-6: Sensor locations in heater boreholes (top view)

4.2.8 Microseismic Measurements (optional)

As a result of the excavation of niche 4 and the drilling of the two large-scale boreholes for the heaters and of the numerous monitoring boreholes, the formation of a complex excavation damaged zone (EDZ) in the floor of the niche and in the walls of the large-scale boreholes is to be expected. During the course of the experiment, further deformation of the Opalinus clay due to the temperature input of the first heater is expected.

Using microseismic measurement methods, the rock mass is to be seismically characterised regarding the changes to be expected. This will be done in representative areas and at different points in time, starting before the first heating phase begins. To this end, interval velocity measurements (IVM) will be performed in various directions in the large-scale boreholes and 4 cross-hole measurements (XHM) will be performed between monitoring boreholes BS1-4 (Figure 4-7).

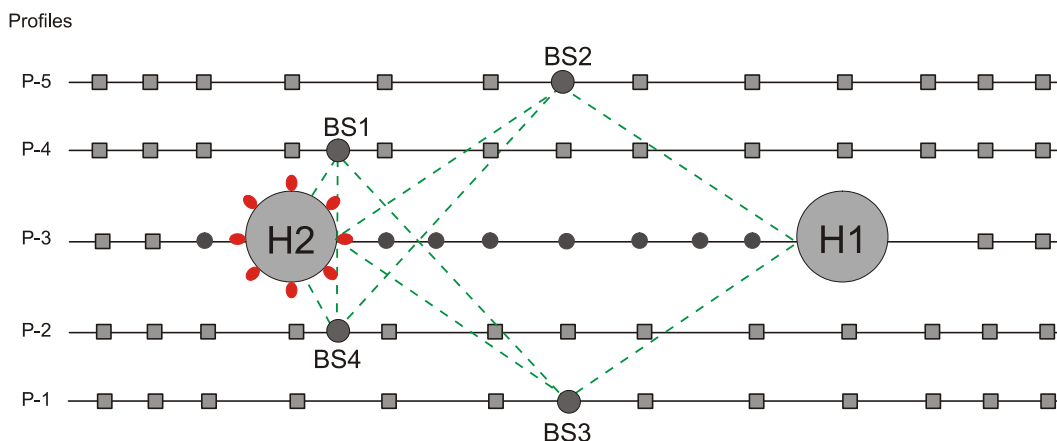


Figure 4-7: Paths of rays during the microseismic measurements

For the seismic characterisation of the Opalinus clay, Sv wave velocities, amplitude dampings as well as dynamic, pseudoelastic parameters, e.g. Young's modulus, Poisson's ratio, will be deduced from these data. These data can be used to estimate the degree of damage and the spatial extent of the EDZ. The parameters derived from repeated measurements allow the prediction of time-dependent changes in the rock mass that are due to the temperature input and potentially occurring stress redistributions.

4.2.9 Installation of Heater 2 and of the SB Buffer Material

After the first heating phase has been completed, the second borehole will be equipped with the second heater which is subsequently connected and subjected to a function test. As was the case with borehole 1, the borehole wall of borehole 2 will be equipped with temperature sensors along 4 vertical profiles. The void space around the heater will be filled with bentonite-sand granules which will be slightly compacted. Subsequently, the void above the heater up to the floor of the niche will also be backfilled with bentonite-sand granules which will be compacted in layers. The borehole will then be sealed by means of a steel plate which will be fastened to the floor of the niche.

4.3 Experimentation

After all preparatory measurements have been completed, the heater in the first borehole will be started which marks the beginning of the actual experiment.

4.3.1 Heating Phase 1

During heating phase 1, it is intended to heat the first large-scale borehole for 1.5 years. Design calculations performed in the previous study show that during this period the temperature at the second borehole will reach a level that corresponds to the temperature in a real borehole being prepared for emplacement. During this period, the THM behaviour of the rock mass will be monitored by means of the geotechnical measurement systems. The second large-scale borehole will remain open during this period while borehole deformations due to the thermally-induced mechanical load will be monitored and recorded. All measurement data of all sensors will be made available to authorized users on a website set up for this purpose. The company SolExperts has been selected for the data recording and their posting on the internet. The measurement results will be visualised and analysed and documented in raw data reports at regular intervals.

In addition to the geotechnical measurements of the THM behaviour of the rock mass, microseismic measurements are intended to be performed by BGR at regular intervals. These measurements are to detect any changes in the rock mass between the two large-scale boreholes identifiable by changed propagation speeds of the seismic waves and, if possible, to correlate these changes with the geotechnical measurements. Microseismic measurements will also be performed in the second, open large-scale borehole in order to detect any changes in the excavation damaged zone.

4.3.2 Heating Phase 2

After conclusion of heating phase 1, the second, still open large-scale borehole will be equipped with a heater. Temperature sensors will be installed and the bentonite-sand buffer will be filled in. During this second heating period both large-scale boreholes will be heated for a further 1.5 years. During this period, the monitoring of the THM behaviour of the rock mass by means of the geotechnical measurement systems will continue. Especially the interaction between the temperature fields is to be monitored. At the same time, the mechanical load on the canister dummies (heaters) will be monitored and recorded. The posting of all measurement data of all sensors on a website set up for this purpose will continue. The measurement results will be visualised and analysed and documented in raw data reports at regular intervals.

4.3.3 Cooling Phase

The experimental design also comprises a defined cooling phase. According to the current concept, this phase is scheduled for 3 months. It is assumed that after this period, the temperature of the rock mass will approximate the initial temperature again, i.e. before heating.

4.3.4 De-installation and Follow-up Studies

After completion of the cooling phase, the measurement and heating systems will be de-installed. All sensors that are recoverable will be removed. The bentonite-plus-additive buffer in the two large-scale boreholes will be removed layer by layer. The sensors embedded in the boreholes will be removed, and the two heaters will be retrieved. Finally, the two large-scale boreholes will be backfilled or at least covered by steel plates for safety reasons.

5 Modelling Concept for Experiment Analysis

An important part of this experiment is the mathematical analysis and modelling of all measurement results. Using models, the rock behaviour can be described in a comprehensible manner. The adjustment of constitutive laws and identification of parameters are a basis for the model simulation of the physical processes observed.

5.1 Model Design and Predictive Calculation

After completion of the heater and monitoring boreholes and after installation and verification of the exact positioning of all sensors, a geometric 3D model will be generated and overlaid with a suitable grid. The model geometry is based on the geologic situation, in this case especially on the orientation of the Opalinus clay strata that in the area of the niche destined for the experiment have an inclination of approx. 45°. The model and the grid are generated in such a way that all sensors can be integrated in a suitable way as monitoring points in order to obtain a model that reflects their positions as precisely as possible.

In a second step, a conceptual model will be generated that mathematically describes all rock properties in a suitable way. This model can be based on reference constitutive laws and parameters for Opalinus clay that have been identified within the scope of investigations by NAGRA (NAGRA 2002) and previous laboratory and in-situ experiments. However, it must be kept in mind that these laws and principles are primarily valid for clayey and not for sandy facies. Corresponding modifications for a sandy facies are thus to be expected.

When both models have been completed, test calculations will be performed in order to demonstrate the functionality of the models. Finally, predictive calculations of the THM behaviour of the rock in accordance with the current experimental design will be carried out.

5.2 Modelling During Phase 1 of the Experiment

When sufficient data are available for comparison with the model calculations, the predictive calculations will be reviewed. Conformities and discrepancies will be analysed and, where necessary, parameter adjustments will be made before a new predictive calculation for the remaining course of the experiment in phase 1 will be run. This process will be repeated at regular intervals in order to simulate the THM processes in the model as precisely as possible.

The modelling will be accompanied by statistical analyses that, in view of the multitude of temperature sensors, are to provide the means to detect any implausible measurement results of individual sensors and to eliminate these from the comparison process between model calculation values and measurement values. This is to increase the accuracy of the parameter adjustment, especially of the thermal parameters.

5.3 Modelling During Phase 2 of the Experiment

The set of data and parameters identified within Task 4.2 (phase 1) will be used as an initial data set to start the simulation of phase 2 in order to also obtain a first prediction of the second heating phase. Again, when sufficient data are available for comparison with the model calculations, the predictive calculations will be reviewed. Conformities and discrepancies will be analysed and, where necessary, parameter adjustments will be made before a new predictive calculation for the remaining course of the experiment in phase 2 will be run. This process will also be repeated at regular intervals in order to improve the simulation of the THM processes in the model.

The modelling in the second phase will also be accompanied by statistical analyses in order to detect any implausible measurement results and to eliminate them from the comparison process between model calculation values and measurement values. By means of an error analysis using the method of least squares and using all sensors, an optimal set of parameters for the sandy facies of the Opalinus clay is to be identified.

5.4 Modelling During the Cooling Phase

At the end of both heating phases, an optimal set of parameters for the sandy facies of the Opalinus clay will be available. After both heaters have been turned off, this set of data is to be verified by means of a comparison between predicted and measured values.

6 Experiment Cost Estimate

One objective of this study was to deliver a realistic cost estimate of the experiment that allows the preparation of a well-founded proposal for funding. The description of work given in chapters 4 and 5 was used as a basis to identify qualified institutes or companies having the capabilities to perform the work in a reliable and most efficient manner. As a result, the following suitable subcontractors have been identified:

Geotechnical Institute (Switzerland)	On-site management
COFOR-COREIS (France)	Drilling of heater and extensometer boreholes
Aitemin (Spain)	Development, fabrication, installation, operation, and maintenance of the two heaters
SolExperts AG (Switzerland)	Geotechnical Measurements: Production, installation, operation, and maintenance of the sensor systems (except pore water pressure system) as well as data recording, data documentation and website management
Geoph.-Techn. Büro Clausthal (Germany)	Laboratory and in-situ determination of thermo-physical properties of the Opalinus clay and buffer material investigation
Swisstopo (Switzerland)	Measurement of uplifts due to heating in the experiment niche

Qualified quotations have been obtained from these potential subcontractors to get realistic information about the necessary budget.

The drilling of the small monitoring boreholes and the installation and operation of the pore water pressure sensor system will be performed by our project partner GRS. In addition, GRS intends to do laboratory investigations on their buffer material and additional numerical simulations. A cost estimate for this work will be provided by GRS in a separate report. The geophysical (microseismic) measurement campaigns planned by BGR are not included in the cost estimate except the special carrier that has to be developed in order to lower down the measurement devices into the heater boreholes. Table 6-1 summarizes the calculated budget for the work described in chapters 4 and 5. Overhead costs and VAT are not included.

Table 6-1: Necessary budget for the TwisT experiment

Type of Work	Costs (€)
Laboratory investigations	21 580
Experiment preparation and preparatory measurements	1 151 140
Experimentation	452 000
Mathematical modelling and analyses of test results	226 400
Documentation and reporting	68 300
Total	1 919 420

7 Conclusions

In the framework of this feasibility study a detailed concept for the TwisT experiment has been developed. As a result of design calculations, a suitable experiment configuration was obtained that ensures a most accurate and efficient process monitoring during experimentation. For the thermal, mechanical, and hydro-mechanical processes, the main results of the calculations are summarized as follows:

Thermal design:

- Heater power:
When applying a power of $P_1 = 968 \text{ W}$ and $P_2 = 711 \text{ W}$, the design temperature of 100°C at the contact surfaces bentonite/heater is not exceeded.
- Borehole spacing:
For a borehole-to-borehole distance of 6 m (and the above mentioned heater power), the thermal influence at borehole 2 caused by the heating of borehole 1 does not exceed the admissible temperature increase of 2 – 4 K, which corresponds to former repository design calculations.

Mechanical effects:

- Niche displacements
The smallest displacement is calculated for the niche walls, whilst the niche floor shows the largest displacements. The displacements range from 0.4 mm (reference model, drift wall) to 8.6 mm (creep model, drift floor).
- Borehole convergence
The calculated displacements are up to 1.5 mm at the end of the calculation period (730 days). A deformation of the borehole contour occurs due to elasto-plastic response, to thermal expansion as well as due to creep behaviour. Directly after drilling, the elasto-plastic response results in an instantaneous reduction of the borehole diameter. At the borehole mouth (EDZ of niche floor), the plastic deformation causes significant widening of the borehole perpendicular to the niche axis and constriction parallel to the niche axis.
After the start of heating at borehole 1, the contour of borehole 2 is changed: (i) the thermal expansion results in a displacement of the borehole in a direction away from heater 1, with greater displacements on the side facing borehole 1, and (ii) a further extension of the EDZ is observed.
- Borehole stability
Below the EDZ of the niche, the borehole remains stable during the entire simulation in the reference model and the creep model. In the elasto-plastic model with reduced strength properties, yielding occurs in the borehole close to the heater.
- Maximum stress acting on the heater surface
Heater 1 $\approx 1.7 \text{ MPa}$ (granular bentonite), 9.1 MPa (highly compacted bentonite)
Heater 2 $\approx 1.6 \text{ MPa}$ (granular bentonite), 7.7 MPa (highly compacted bentonite)

At the time being, it is intended to use granular bentonite with slight in-situ compaction.

Hydro-mechanical effects:– Expected maximum pore pressure

The maximum pore pressure occurs at heater 1 after 30 days of heating. The following pore pressures were calculated by means of the different mechanical models:

- reference model: ~ 3 MPa
- elasto-plastic model with reduced strength properties: ~ 2.7 MPa
- creep model: ~ 3 MPa

– Influence / disturbance of pore pressure field

Prior to heating significant drainage of the host rock occurs. At a depth of 3.6 m below niche level (expected middle of heater) the pore pressure drops to ~1 MPa (initial value: ~2 MPa). The larger the EDZ around the cavities (niche and boreholes) the lower the maximum pore pressure during the simulation because a larger EDZ allows for faster drainage so that the pore pressure increase caused by heating is partly relieved. The elasto-plastic model with reduced strength properties has the largest EDZ, and accordingly it has the lowest maximum pore pressure (2.74 MPa). The creep model exhibits the smallest EDZ and the highest maximum pore pressure (2.99 MPa).

– Evolution of pore pressure

The maximum pore pressure occurs 30 days after starting the heater operation. A second maximum occurs due to the start of heater 2. Afterwards drainage and an equilibration of the pore pressure field dominate. During the calculation period (730 days), the steady-state pressure field is not reached.

– Borehole stability

The heating at one borehole affects the pore pressure at the adjacent borehole. But the influence is small compared to the maximum pressure changes which occur close to the operated heater. At a depth of 3.6 m, stability is predicted and failure could only occur within the EDZ and close to the heater at a depth of 3.65 m when applying reduced strength properties.

– Saturation of buffer

Only the periphery of the buffer is fully saturated and a peripheral zone of a few cm within the buffer is partly saturated at the end of the experiment.

The results of the design calculations allow the identification of the most suitable monitoring devices to ensure that all relevant physical processes during the experiment can be measured as precisely as possible. The experiment configuration, the test schedule and work flow has been developed so as to investigate best possible the THM interactions occurring during the experiment. Based on the experiment design, the necessary work and the qualified quotations, the budget for the TwisT experiment (excluding GRS budget) has been calculated to be about 2 Mill. Euro plus overhead costs and VAT.

8 References

ANDRA 2005

Premiers enseignements de l'expérimentation HE-D Au Mont Terri, Période Septembre 2003 à octobre 2004, Y. Wileveau, Laboratoire de Recherche Souterrain de Meuse/Haute-Marne, Rapport, Document interne, ANDRA, 2005

GRS 2004

Thermo-Hydro-Mechanical and Geochemical Behaviour of the Callovo-Oxfordian Argillite and the Opalinus Clay. Final Report. Zhang, C.L., Moog, H. Dittrich, J., Müller, J.. GRS – 202. June, 2004

Hoth et al. 2007

Untersuchung und Bewertung von Tongesteinsformationen, Endlagerung radioaktiver Abfälle in tiefen geologischen Formationen Deutschlands. Hoth, P., Wirth, H., Reinhold, K., Bräuer, V., Krull, P. und Felldrapp, BGR Berlin/Hannover, 2007.

Jobmann et al. 2007

Untersuchungen zur sicherheitstechnischen Auslegung eines generischen Endlagers im Tonstein in Deutschland. GENESIS. Abschlussbericht. Jobmann, M, Uhlig, L., Amelung, P., Billaux, D., Polster, M., Schmidt, H.. DBE TECHNOLOGY. März, 2007

Jobmann 2008

Untersuchungen zur Auswirkung einer Temperaturbelastung auf Tonformationen in Deutschland im Nah- und Fernfeld. TEMTON. Jahresbericht 2007. Jobmann, M., DBE TECHNOLOGY, Januar, 2008

NAGRA 2002

Projekt Opalinuston, Synthese der geowissenschaftlichen Untersuchungsergebnisse. NAGRA. Technischer Bericht 02-03. Dezember, 2002

Rothfuchs et al. 2005

Self-sealing Barriers of Clay/Mineral Mixtures in a Clay Repository - SB Experiment in the Mont Terri Rock Laboratory, Final report of the Pre-Project, Rothfuchs, T., Jockwer, N., Miehe, R., Zhang, C.-L., GRS - 212, Gesellschaft für Anlagen und Reaktorsicherheit, (GRS) mbH, Köln, 2005..

SKB 2008

Temperature Buffer Test, Sensors data report (Period 030326-080101, Report No: 11). SKB. IPR-08-16. January, 2008

Uhlig et al. 2007

Untersuchungen zur sicherheitstechnischen Auslegung eines generischen Endlagers im Tongestein, F+E-Vorhaben GENESIS, Abschlussbericht. Uhlig, L., Amelung, P., Billaux, D., Jobmann, M., Polster, M., Schmidt, H., DBE TECHNOLOGY, Peine, 2007.